



**HAL**  
open science

# Glass, pottery and enamelled objects: identification of their technology and origin

Philippe Colomban

► **To cite this version:**

Philippe Colomban. Glass, pottery and enamelled objects: identification of their technology and origin. Conservation Science: Heritage Materials, 2nd Edition, P. Garside & E. Richardson Eds, RSC, 2020, 978-1- 78801-093-1. hal-03622849

**HAL Id: hal-03622849**

**<https://hal.science/hal-03622849>**

Submitted on 29 Mar 2022

**HAL** is a multi-disciplinary open access archive for the deposit and dissemination of scientific research documents, whether they are published or not. The documents may come from teaching and research institutions in France or abroad, or from public or private research centers.

L'archive ouverte pluridisciplinaire **HAL**, est destinée au dépôt et à la diffusion de documents scientifiques de niveau recherche, publiés ou non, émanant des établissements d'enseignement et de recherche français ou étrangers, des laboratoires publics ou privés.

## Glass, pottery and enamelled objects: identification of their technology and origin

Philippe Colomban  
Sorbonne Université, CNRS, MONARIS umr8233  
4 Place Jussieu, F-75005 Paris, France  
[philippe.colomban@sorbonne-universite.fr](mailto:philippe.colomban@sorbonne-universite.fr)

### Abstract

Much like weapons, vessels made from glasses and ceramics have long been held as objects of very high technology. Ceramic technology mastery is even at the foundation of metallurgy. In producing glass, potteries and enamelled metals, three critical, and energy intensive steps are needed : obtaining fine powder, firing, and building appropriate kilns. Control of the colour also requires advanced physical and chemical knowledge. Indeed, if ceramic production is somewhat the art of forming a heterogeneous matter (only some components melt), glass or enamel production requires the object to pass through a homogeneous liquid state to obtain the desired microstructure and properties. This chapter presents the different destructive, non-destructive and non-invasive analytical methods that can be carried out in laboratory, on shards or sampling with fixed 'big' instruments, or on site (museums, reserves, etc.) with mobile set-ups. After a brief overview of the history of pottery, the implications of the processes involved (grinding, shaping, sintering, enamelling, decoration) on micro- and nano-structures (formation / decomposition temperature, kinetic / phase rules, sintering) is given. The emphasis is given to information that can be obtained by XRF and Raman mobile non-invasive measurements. Examples illustrating how these studies help to document technology exchanges and exchange routes are also given.

### 1. Pottery and enamelled artefacts. Definitions and brief historical overview

The mastering of fire is associated with the early development of Mankind. The first potteries appear to have been produced as early as 12,000 BC in different continents (Japan, Siberia, Africa), before or just at the Neolithic Transition from nomadic to sedentary life.<sup>1-6</sup> However, artefacts made of fired clay are much older (about 25-30,000 BC for the Dolni Vestonice Venus sculpture).<sup>7</sup> The first potters could have been itinerant, as pointed out by archaeological and ethnographic studies,<sup>8</sup> and their main activity may have been the production of containers of differing shapes. The word *pottery* is coming from Latin *potum*, the name of a drinking utensil. *Ceramic* is coming from the Greek *keramos* (*κεραμος*) which means *horn*, indicative of the matter then used for drinking utensils. *Glass*, *glaze* and *enamel* (and smalt) are thought as coming from the Proto-Germanic '*glasa*' (to shine) and '*smaltjan*' (to smelt), respectively. In Chinese language the word for pottery, *tao ci* (陶器), is related to a more philosophic meaning: *the way*, the principle of life, and this fact could explain the importance of Ceramic Art in Asian Cultures. A good knowledge of pottery and enamelling technologies is needed to analyse ancient artefacts. Here we will try to give an overview of the background required, as well as useful references.

Ceramic tools were required for the development of metallurgy and both techniques require the building of kilns and the careful selection of raw materials. **Fig. 1** schematizes the technological evolution from the production of pottery consisting in a porous body, free of waterproofing coating, up to an advanced high dense porcelain enamelled with a complex décor, and then to special ceramics and glass having specific chemical, thermomechanical or electrical/magnetic properties.<sup>5,6</sup>

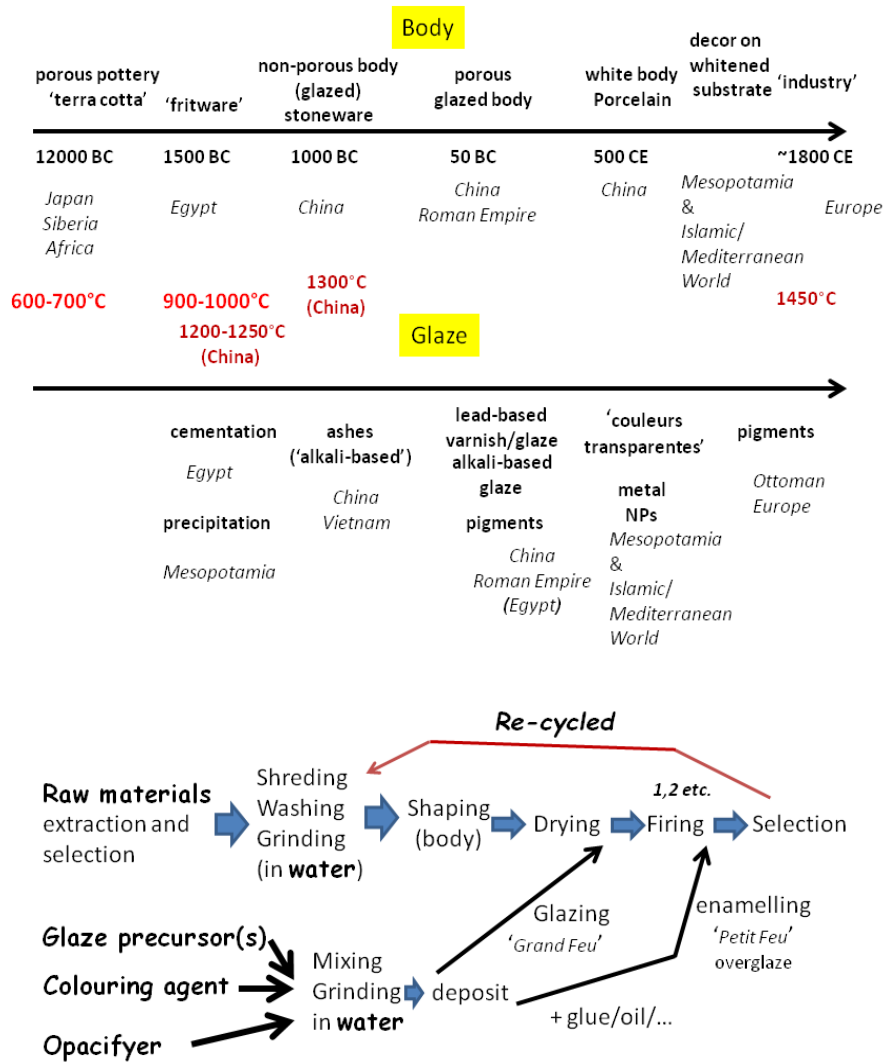


**Fig. 1.** Timeline of the development of pottery technology. Required firing temperatures are indicated in red. The development of technologies associated with kiln production determines the evolution of ceramic production. Diagram of a ceramics manufacturing cycle.

The deposit of a waterproofing coating, a glassy silicate called 'glaze', only started with the development of an urban culture/élite in Egypt and Mesopotamia, ca. 1500 BC. Preparation of glassy paste is much older.<sup>3-6</sup>

The first classification of the different types of pottery (**Table 1**) was established in 1844 by Alexandre Brongniart, head of the French Imperial (established as a Royal Factory by Louis XV in 1756, then as National Factory during French Revolution and presently) Sèvres Factory and in 1805 founder of the first Ceramics Museum coupled to a Factory.<sup>9,10</sup> Brongniart's classification is based primarily on the mechanical properties of the fired body and on the composition of the glaze. This slightly modified classification (**Table 2**), remains the reference to this day.<sup>11,12</sup>

Consequently, studies conducted on ancient pottery and enamelled artefacts (on glass or on metal) are aimed at documenting technical history and production methods, identifying characteristics related to:

- i) the raw materials (nature, provenance, selection, processing (washing/grinding/heating))
- ii) the body and its processing/firing (microstructure, phases, compositions)
- iii) the decor/coating (nanostructure, composition, colouring agents, pigments)

- iv) the firing cycle and kiln technology (fuel, casing ...)
- v) the relationship with other/previous centres of production.<sup>2-6</sup>

Such information informs our understanding of trade routes and technology transfers.

**Table 1:** Types of pottery (after Brongniart' classification)<sup>9,10</sup>

Class	Type	Glaze	Remarks
Soft-paste body	Terra cotta	no	-
	Lustre pottery	Silica-alkaline composition	Thin 'coloured' glaze
	Varnished pottery	Lead-rich composition	
	Glazed pottery (faience)	Tin oxide opacification	
Hard-paste (non-fuse) body	Fine faience	Lead-based composition	Colour-less body
	Grès-cérame (stoneware)	No or silica-alkaline composition	Coloured body
Hard-paste (translucent) body	Hard-paste porcelain (China)	Feldspar-based composition	Use of Kaolin
	Soft-paste 'natural' porcelain (fritware, English bone China)	Lead-(borax-) based composition	Use of clays or kaolin or bones
	Soft-paste 'synthetic' porcelain (fritware)	Lead-based composition	Use of marl and frit

**Table 2:** Professional classification of ceramics<sup>11,12,34</sup>

Class	Type	Body open porosity %	Glaze	Remarks
<b>terra totta</b>		20-35	No coating	
	Varnished/glazed		Lead-based	
<b>Faience</b>		15-20	Tin oxide opacification	
	Fine faience	10-15		Colourless body
<b>Fritware</b>		<15	Lead-based	A slip can be added in-between body and glaze
<b>Stoneware</b>	Salt varnish vitreous	<5	Alkaline (Salt)	
		<3	Feldspar based	White body
<b>Porcelain</b>	Hard-paste (China)	<1		Feldspar & kaolin-based body
	Bone China	<1		Phosphate-based body
	Soft-paste	<2	Lead-based	Vivid colours
<b>Technical</b>	Oxide	<0.5	In general, no glaze	Physical/chemical properties controlled
	Carbide			
	Nitride			
	Carbon			

The interest in the documentation of technologies is long-standing. A first foray in the matter can be found in Pliny the Elder's History.<sup>13</sup> A few rare medieval manuscripts dealing with the subject have survived, such as those of Theophilus,<sup>14</sup> del Rey Alphonso<sup>15</sup> or Jean d'Outremeuse<sup>16</sup> in Western countries and those of Persian potters in the Islamic World.<sup>17,18</sup> Subsequently, the development of the printing press led to an abundance of books concerning the Fire Arts during the 16<sup>th</sup> century,<sup>13</sup> in particular those of Agricola, Piccolpasso, Neri, etc.<sup>13,19,20</sup> The technical literature was then broadened during the 18<sup>th</sup> century.<sup>21-23</sup> The first archaeometric studies on porcelain were published by François de Réaumur,<sup>23</sup> in light of the information collected in China by Jesuit d'Entrecolles, during his visit of the Jingdezhen Factory, one of the leading Chinese centres in porcelain production.<sup>24</sup> The interest at

that time for all Fine Arts techniques was large as proved by the publication of the Encyclopédie.<sup>25</sup> However, it is with the works of Brongniart,<sup>10</sup> Bastenaire-Daudenart (especially in faience)<sup>26</sup>, Brongniart and Bontemps (glass)<sup>27,28</sup>, and then of Salvetat,<sup>29</sup> Deck<sup>30</sup> and others<sup>31-34</sup> that very useful technical and scientific reference books became available. More details can be found in reference<sup>13</sup>.

## 2. Raw materials and processing (grinding, shaping, firing, enamelling)

We will first define some terms. Raw materials are the rocks selected for the preparation of the artefact (unfired or 'green' ceramic body) and of the glaze/glass/enamel precursor (**Fig. 1**). A rock is generally the association of different minerals: for instance, a pegmatite (*petungtse*) is a rock made of big crystals of feldspars, quartz and micas. The composition of minerals is very variable and the composition of centimetre-long feldspar crystal can vary from potassium-rich (orthoclase or microcline) at one tip to sodium- (albite) or calcium-rich (anorthite) solid solution at the other one. Clays are (earth)alkali aluminosilicates in the form of lamellar nanoparticles, the interlayer cations being more or less solvated by water molecules. A clay (rock) can be made of different clayed minerals (illite, smectite...). Kaolin (rock) and associated mineral (kaolinite) belong as clay to phyllosilicate group but do not have interlayer (earth)alkali cations and hence a much higher melting temperature than clays and a much lower plasticity. To eliminate impurities that can colour the matter, raw materials are carefully washed (and mixed and stored) before use.

Artefacts are prepared by hand(wheel)- or mould-shaping from clay-based paste (water content ~20-30% wt).<sup>10-12,34</sup> Addition of water led to an aqueous suspension (sol) that can be used to make vessel using a porous (plaster) mould; part of water is trap, and a millimetre-thick layer form at the mould surface by sol-gel transition; pouring of remaining liquid slip and drying allows recovering the green body. Complete drying and firing are then performed.

Enamel is a glassy coating on a substrate, metal or ceramic; a glaze is an enamel on a ceramic body; French terms '*glaçure*' and '*couverte*' correspond to a glaze on a porous body (and hence deposited on already fired body) and on porcelain/stoneware/vitreous (deposited on 'green' body and fired at the same time). A frit is a mixture melt and quickly cooled in water in order to make easier powdering of the resulting glassy mixture. Frit can be used as ingredient of body (fritware/stonepaste/softpaste) and glaze (**Tables 1 & 2**).

The number of raw materials required to produce pottery, glass/glaze and enamelled artefacts is variable. For *terra cotta* and certain faience and stoneware only one 'clay' was used. However, in the majority of cases the addition of sand is required: the large shrinkage of the clay-water mixture (typically 30 wt% water is needed to obtain a paste ready for shaping<sup>11,12</sup>) requires the mixing of the clay with an inert phase to avoid the formation of 'elongated' cracks during the drying. Broken and powdered ceramic waste (also called fired clay) can replace partially sand. In a sand- or fireclay-containing paste, small shrinkage-cracks form around inert grains that prevent the formation of long cracks. These small cracks disappear during the firing/sintering stage. More complex potteries require the use of different clays, each of them giving specific properties: good plasticity for shaping, good mechanical strength in the green state (i.e. before firing), good sintering, etc.<sup>11,34</sup> For sophisticated ceramics such as fine faience and porcelain many clays/kaolin, feldspar and sands are used.

Consolidation during firing (called 'sintering') results from the reaction between adjacent grains. A liquid phase forms at the grain surface and accelerates reaction kinetics (atom diffusion rates are order of magnitude faster in liquid state and dissolution-precipitation phenomena at the corrugated surface of grains help to form cement in between adjacent grains, **Fig. 2**). A good compaction of clay, sand, and feldspar grains maximizing the number of inter-grain contact is mandatory to obtain a good sintering and low porosity artefact with good mechanical properties. Contrarily to glass preparation that requires the melting of the entire batch, ceramics are achieved with a limited

volume of molten phase: fluxing materials such as chalk, feldspars, intrinsically, or by contact, melt at low temperature (<1100°C). Addition of frit, lead oxide, borax, iron oxide, etc. lower the melting temperature up to 500-700°C.

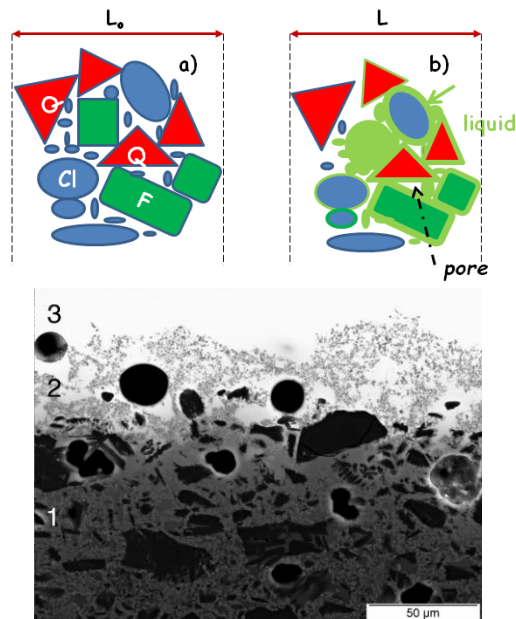


**Fig. 2:** Sketch of the transformation taking place during the sintering: a) compacted matter; b) a liquid phase forms, wets the grains and cements them on cooling (Q: quartz, F: feldspar, Cl: clay aggregates); the densification ( $L < L_0$ ) and the formation of new phases, amorphous and crystalline on cooling cements the grains; c) SEM-BSE photomicrograph of a cross-section from the body (1) to the Pb-rich glaze (3) with a reaction zone (2) in between. The body shows some large roundish pores (black), relictic quartzes surrounded by circular cracks (black), subidiomorphic tridymite laths (black), many small subidiomorphic crystals of wollastonite (white) and a glassy matrix (grey). The outermost parts of the body lack wollastonite and is also part of the reaction zone. The 1-2.5  $\mu\text{m}$  long, prismatic shaped and CaO-rich crystals (grey) of the reaction zone are too small for a quantitative chemical analysis. Soft (frit) porcelain plate from the Royal manufacture of Sèvres, France, 1781 (Courtesy of Prof. M. Maggetti, see ref. 93 for details).

In order to decrease the amount of undesirable phases (colorant, source of gas) and/or to avoid coarse grains, grinding, washing and flotation can be made. Kaolin and clays are rocks formed by the corrosion and sedimentation of mother rocks such as gneiss, granites, pegmatites ... (a mixture of feldspars, quartz, and micas). This led to naturally fine grain materials (largest dimension ranges from a few nanometer to a few micron) but composition in a quarry varies from place to place. Deterioration of the quality of the production of a factory, and then its disappearance, results often from the impossibility of the potter to adapt the processing to the shift of the composition. Specific trace elements (Sr, Rb, rare earths, U, etc.) or minor components (Fe, Ti, Zr, etc.) can be used to identify particular raw materials with the same provenance.<sup>35-41</sup> The more sophisticated the technology of production, the easier will be the identification of place or date of production. Indeed, innovations can be used as *post quem* milestones.<sup>13</sup> As an example **Fig. 3** shows the plot of the Rb vs. Sr and Ti vs. Fe content measured with a portable X-ray fluorescence (pXRF) instrument in the body of 'Boccaro' wares (early 18<sup>th</sup> century red stoneware assigned to J.F. Böttger, Meissen, Saxony).<sup>36,37</sup> Data have been normalized to the Si signal in order to take into account the variation of geometrical conditions of measurement, such as distance and angle of analysis, owing to the different shapes of the objects. These 'Boccaro' wares try to imitate *Yixing* Chinese contemporary productions, highly prized by the European élite of the 17<sup>th</sup> and 18<sup>th</sup> centuries.<sup>36,37</sup> For instance some teapots have been prepared by moulding the original *Yixing* wares and confusion was possible when employing only visual criteria to distinguish them.<sup>36</sup>

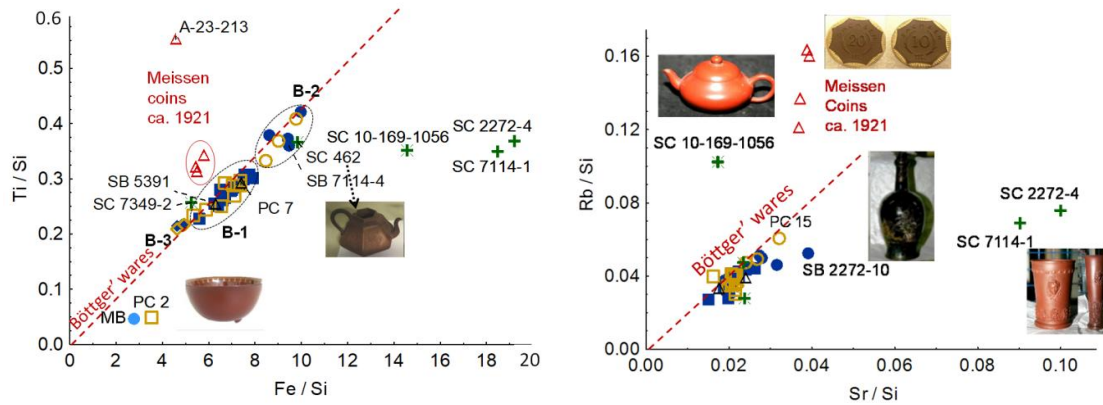


**Fig. 3:** Examples of categorization obtained from the elemental ratio plots, here measured with a portable XRF instrument (after<sup>36</sup>); Böttger' productions made with the same raw materials providing Rb and Sr, or Ti and Fe element ratio are located along the straight line starting from the origin. Other artefacts are Chinese, modern Meissen and fake items.

Matter made with variable proportions of the same raw materials will give data aligned on a straight line starting from the origin. For instance, Rb and Sr elements are associated with calcium (from chalk or alabaster or gypsum) and Ti and Fe elements are typical impurities of clays and kaolin. Differentiation between Böttger, aligned with the calibration line, and Chinese *Yixing*, modern Meissen and other artefacts is thus obvious.<sup>36,37</sup> For instance the SC462 tea-pot from Sèvres Collection was a true Böttger 'Boccaro', whereas the SC 10-169-1056 was actually the Chinese model. These elements have been selected by considering the impurities *a priori* characteristic of the raw materials reported to have been used at Meissen (red kaolin, alabaster, etc.).<sup>42,43</sup> Another approach is the use of algorithmic techniques such as principal component analysis (PCA), Euclidean cluster variation method, supervised PCA<sup>44</sup>, to identify the most pertinent parameters, statistically and independently of the considerations regarding the ceramic or glass technology. The preparation of enamels requires the availability of fine (micronic or submicronic) powder(s).<sup>45</sup> Grinding needs a lot of energy and before the mastering of hydraulic energy (~12<sup>th</sup> century in Western Europe, 9<sup>th</sup> century in the Islamic World), potters and glassmakers took advantage from the thermal decomposition of 'hydrated' compounds to obtain fine powders: for example  $\text{Ca}(\text{OH})_2$  from calcareous rocks or shells, calcium phosphate from bones and complex compositions ready for glazing from wood and plant ashes.<sup>45-47</sup>

The main mechanism of the sintering of pottery is the so-called liquid sintering<sup>11</sup>: at a given temperature one of the raw materials melts, or at the contact between two different raw materials, a liquid phase appears, although the other component grains are not modified.<sup>11</sup> Sintering takes place (Fig. 2): first, the liquid phase dissolves corrugations at the grain surface; the liquid phase forms a neck between grains in contact, forming cement on cooling with the precipitation of new phases, and promotes a densification due to the rearrangement of the grains by capillarity/wetting effect.<sup>11,12</sup> Figures 2a and 2b show a sketch of the body microstructure before and after formation of a liquid phase by reaction between feldspar grains and clay aggregates. The liquid phase wet the grains, forming liquid necks in between that bring by capillarity the grains closer. Dissolution of small grains and corrugations modifies the liquid composition, and led to new phases that precipitates; the composition of the liquid phase also evolves toward less fusible composition, the liquid phase becomes more viscous and solidifies. A bridge is formed in between adjacent grains. The Figure 2c shows the polished section of a glazed porcelain observed with scanning electron microscope (SEM); the backscattered electron (BSE) mode is sensitive to the Z number (matter made of heavier elements appears whiter). At the contact between molten glaze and solid substrate, part of the body

is dissolved, saturates the glaze and small crystals appear. In some cases, the liquid glaze can separate into two liquid phases that led to opalescent glaze (see further).

Everybody can experiment the efficiency of a liquid phase to facilitate densification: a hard and dense ball of snow is easily obtained with snow at temperature close to 0 °C (water –assisted densification); on the contrary it is almost impossible to make a ball with cold snow (-15 °C or more).

Hydroxylated compounds (as clays) undergo dehydration/decomposition around 600 °C, giving a very reactive and fine material (called metakaolin if kaolinite are present).<sup>11,45</sup> The first liquid phase forms at about 750 °C between silicates and FeO-Na<sub>2</sub>O,<sup>48</sup> i.e. in a reducing atmosphere and reacts with the high reactive product arising from clay/kaolin deshydroxylation. *Terra cotta* with rather good mechanical strength<sup>49</sup> can be thus obtained millennium ago with very simple kilns made from pits covered with branches and straw.

Lead oxide melts at ~900 °C, but addition of alkali or alkaline earth-rich materials or borax melt at lower temperature, as low as about 500 °C.<sup>48</sup> Most of the liquid phases of SiO<sub>2</sub>-Al<sub>2</sub>O<sub>3</sub>-CaO-Na<sub>2</sub>O-K<sub>2</sub>O- etc. form between 900 and 1200 °C,<sup>48</sup> the typical range of temperature needed to produce pottery. Wood and plant ashes, a mixture of earth-alkali and alkali hydroxide with small amount of silica and phosphorus oxide were the first glaze precursor.

For instance, typical oxide compositions of faience are given in **Table 3**. Potters do not use actually elemental compositions because the raw materials are natural rocks or minerals and precise composition measurements date from 19<sup>th</sup> century. They use mass (% wt.) or volume (% vol.). A typical composition of faience is clay (26 % vol.), marl (a mixture of clays and limestone, 50 % vol.) and clayish sand (25 % vol.); another example: clay 60 % vol., sand 20 % vol. and limestone 20 % vol.<sup>34</sup> For a (hard-paste) porcelain the proportions are kaolin 50 % wt., feldspar 25 % wt. and sand 25 % wt..<sup>10</sup> This almost correspond to 70 % wt. SiO<sub>2</sub>, 26% wt. Al<sub>2</sub>O<sub>3</sub> and 4 % wt. K<sub>2</sub>O. Regarding phase content, (undissolved) quartz ~22 % vol., mullite (see further) 16 % vol. and glass 62 % vol.

During the sintering of a pottery, only a limited part is molten, from a few vol. % or less for a *terra cotta* up to ~60 vol. % for porcelain.<sup>11,12,50</sup> Porcelain requires temperature higher than 1250°C-1300°C (up to 1450°C) for the growth of long acicular mullite crystals (see further).<sup>50-52</sup> These crystals build a 'bird nest' that retains by capillarity the molten (earth)alkali-rich silicate phase that will give a glassy and translucent phase during cooling. Consequently, a pottery body is always heterogeneous and made of many phases: coarse grains (i.e. relics of raw materials) up to a few millimetres can subsist and new phases resulting from the reaction between the grains form around.

On the other hand, the glassy matrix of enamels and glazes should be homogeneous or its heterogeneity controlled at the micro- or nanoscale.<sup>52-54</sup> Resolution of human eye is close to 1-10 µm; if coloured grains are larger, the colour will appear punctuate, granulated, not united. Three types of colouring agents are used to colour a glass:<sup>53-55</sup>

- i) 3d (transition metal) or 4f (rare-earth) ions having electronic transition in the visible range dissolved in the glassy enamel, as function of the element, 0.05 to 2 % wt are sufficient to colour a glassy silicate.
- ii) Pigments dispersed in the glassy phase or formed by precipitation on cooling. Pigments are crystalline phases coloured by above-mentioned coloured ions not degraded by the molten glass during the process; the coloration power of pigment is higher than that of dissolved ions.
- iii) Metal or semi-conductor nanoparticles with specific organisation or optic properties. The coloration efficiency is huge, 0.2 % wt is sufficient to blacken a millimetre-thick glass plate.



We will discuss further the most suitable techniques to identify the colouring agents.

### 3. Micro/nano-structure and elemental analysis

An exhaustive list is beyond the scope of this publication, but here we try to provide references representative of the different objects and analytical techniques. **Table 3** lists the different methods of analyses and points out some of their advantages and drawbacks. Invasive/destructive methods are commonly used in materials science studies, but we will address those more especially devoted to rare pottery and enamelled objects, which tend to be non-invasive, mobile methods. Glass and ceramics are easily broken and, therefore, artefacts of exceptional quality are very rare so sampling is more often than not prohibited! The use of mobile, non-invasive instruments is needed when shards are not available.<sup>55-64</sup> Optical techniques are optimal for the study of the coloured material. When fragments for sampling are available, scanning electron microscopy with energy dispersive spectroscopy (SEM-EDS) facilities and inductively coupled plasma mass spectroscopy (ICP-MS) are the most used methods to determine elemental composition. ICP-MS, a (micro)destructive technique has for a long-time been to analyse transparent or translucent archaeological glass fragments, available in large numbers and made of a homogeneous matter.<sup>65-68</sup> Some authors neglect the fact that many coloured glazes and even glasses are actually composite materials, and hence the representativeness of the composition probed by ICP-MS can be questioned.<sup>69</sup> The great advantage of advanced ICP-MS is the identification of isotopes.<sup>70-72</sup> For instance Pb isotopes can be used to associate glaze production and mining places.<sup>70</sup> Laser induced breakdown spectroscopy (LIBS) is a microdestructive technique, damaging for enamelled artefacts due to the generation of thermal shock, but offers accurate measurement of composition profiles from surface to body.<sup>73,74</sup> Neutron activation analysis (NAA)<sup>75,76</sup> and ion beam analytical techniques (PIGE: particle-induced gamma-ray emission, PIXE: particle-induced X-ray emission, RBS: Rutherford backscattering spectroscopy, NRA: nuclear reaction analyses) are non-destructive techniques; they can be used to study large objects using an extracted refocused beam line, but instruments are rare and expensive (as well as the transportation of masterpieces from secure room to laboratory).<sup>77-79</sup> Furthermore, the irradiated sample can become radioactive. The microbeam of synchrotron or of rotating anode X-ray sources can be used for local analysis ( $\mu$ XRF or  $\mu$ XRF).<sup>80-85</sup> Transmission electron microscopy (TEM), in particular coupled with focused ion beam (FIB) for the final preparation of the sample, is the unique technique to study microstructure at nanometer and sub-nanometer scale. However, it is expensive and time-consuming to study many samples and therefore the representativeness of the measurements is not obvious.<sup>86-91</sup> XRF, in particular mobile XRF, is a very good method for semi-quantitative elemental analysis.<sup>36-38</sup> Finally, combination of optical and electron microscopies as exemplified in refs<sup>39,92,93</sup> remains the most common approach when fragments are available. The use of vibrational spectroscopies, (FTIR<sup>94-99</sup> and Raman<sup>58-64</sup>) is increasing, not only to identify crystalline and amorphous inorganic phases, but also to identify organic residues in a non-invasive manner,<sup>100</sup> historically made possible by mass spectroscopy and chromatography<sup>101-103</sup> on matter extracted from the pottery pores. These residues inform of the use of the utensils.

**Table 3:** Crystalline phase identification methods. Representative references are given.

Methods	Resolution (usual)	Sample preparation	References
(Polarised) Optical microscopy	0.5-10 $\mu$ m	fracture/cut/polishing	35,38,49,93,113
SEM(EDS)	1-10 nm	fracture/cut/polishing	69,93,132,145
TEM	0.1-1 nm	cut/polished/FIB	86-90
( $\mu$ )XRD	>(10 $\mu$ m)mm	cut/powder	52
$\mu$ XRD (Synchrotron)	1-10 $\mu$ m	cut/polishing	81-84
FTIR-ATR	mm	cut/polishing/powder	94,101
$\mu$ FTIR-ATR	10 $\mu$ m	cut/polishing/powder	102
$\mu$ Raman	0.5 $\mu$ m	No/cut	51,54 (see Table 6)

#### 3.1 Porosity

The first parameter to be considered in the study of pottery is the porosity, the main parameter to classify and name the pottery. The open porosity is commonly measured by the Archimedes method<sup>104</sup>: the comparison of the mass measured in the dry and wet state (pores filled by water under vacuum) with that measured for the wet sample immersed in water, thus allowing calculation of the open porosity.<sup>11,104</sup> Water can be replaced by other fluids for low porosity materials.<sup>105</sup> Closed porosity can be obtained by comparing the density of the sample with that measured with a picnometer on ultrafine powder (the perfect wetting of the powder with the liquid makes the measurement is not distorted by residual porosity), or by comparison with the theoretical density calculated from the unit-cell volume measured by XRD.<sup>11</sup> Typically, open porosity ranges between ~30% for coarse *terra cotta*<sup>49</sup> to less than 0.5% for porcelain<sup>50</sup> and technical ceramics (Table 1). The porosity level directly controls the mechanical properties and the reactivity with the environment. Porous bodies should be enamelled to become tight.

### 3.2 Determining the firing and glazing temperatures

Contrary to crystal and glass that reach a homogeneous state, ceramics, with the exception of single phase technical ceramics sintered after a long high temperature annealing, don't approach the equilibrium state and their microstructures remain very heterogeneous.<sup>108</sup> Much information can be extracted from the microstructure: thus, it is very important to have access to the fracture or the polished cross-section of enamelled artefacts. Pottery is prepared by reactive sintering and the progression of the reactions will be controlled by the degree of grinding, which determines the grain size distribution, and the firing conditions.<sup>11,12,45,108,109</sup> The final quality of a fired artefact depends on the many steps of the process (Fig. 1). Obviously, everybody knows that the cooking of an object in hot water, for instance an egg, depends on both time and temperature, especially at the core; the surface temperature is limited by that of boiling water, whatever the temperature of the heat source. After all water has evaporated, the temperature will depend on the heating. Similar events take place during the firing of a ceramic: for instance, if hydroxides loose water at e.g. 400 °C, the temperature of an untransformed hydroxide grain will be kept at 400 °C up to the complete dehydration, even if adjacent grains are at higher temperature. The same feature takes place for the reaction between a solid phase and a liquid one. Essentially, the composition of the liquid is slightly modified and the viscosity shifts with the dissolution of grains in the liquid phase.<sup>48</sup> Consequently, only the combination "grain size x temperature x time/heating rate" makes sense: for a given value of atom diffusion rate, the matter transportation will be the same if we increase the time or the temperature or if we change their combination (slower heating rate); the area in contact between grain being increased when the grain size decreases, advancement of the reaction will be higher for a compact assembly of fine grains than for one of made coarse grains. This also explains why the core of many grains is preserved in its raw state, with only the periphery and the matter around grains being modified,<sup>108</sup> with appearance of new phases (Fig. 2b). It is thus difficult to reduce the heterogeneity of a ceramic made of coarse and fine grains. Typically, for *terra cotta* and many faience, majolica, etc., sand grains are larger than a few millimetres although the size of clay particles are several orders of magnitude smaller (a few nanometres): the size of new formed phases is thus very variable and a multiscale analysis is required.

As indicated before, grinding, firing and enamelling are critical technologies. The design and construction of kilns were the most critical issues<sup>3-6,110</sup> and the evolution of the techniques shows a progressive increase of the temperature and a decrease of the firing cycle duration. In medieval China firing in Dragoon Kiln lasted many weeks, whereas present day firing duration needs only a few hours or even a few minutes for small artefacts like tiles! The measurement of the thermal expansion/shrinkage of the 'green' body is made by professionals to establish and optimize the heating-cooling cycle.<sup>11,34</sup> **Fig. 4** shows typical curves measured on already fired pieces, a good 'tool' to analyse phase content and to determine the firing temperature of a pottery.<sup>34</sup>

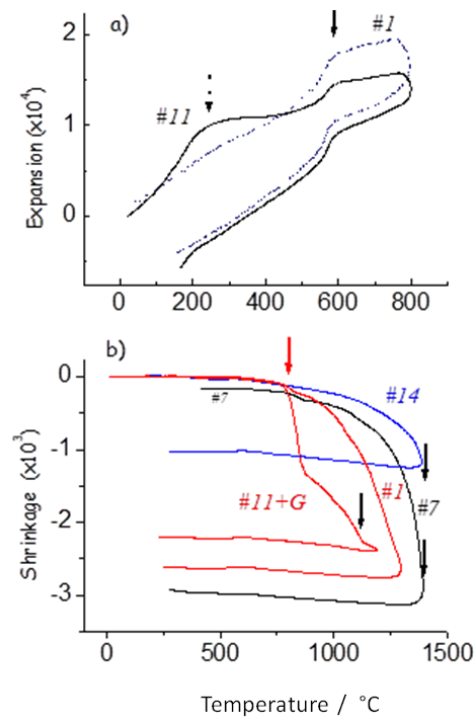


**Fig. 4:** Examples of thermal expansion measured on stoneware/porcelain:<sup>112,113</sup> a) comparison between the thermal expansion of two body of Vietnamese celadons (#1, 13<sup>th</sup> c. and #11 16<sup>th</sup> c. ) heated below their firing temperature: the bumps observed arise from reversible phase transitions of quartz (573°C alpha to beta quartz transition); in b) the shards are heated at higher temperatures; the Y scale is 10 times smaller, so the expansion up to ~800°C appear almost flat; the glazed sample #11+G show a shrinkage jump at the melting temperature of the glaze (arrow), then the slow evolution arises from the reaction of the molten glaze with the body substrate and the second arrow indicates the sintering of the body; the sintering of #7 and #14 16<sup>th</sup> c. Vietnamese porcelains shards takes place at higher temperatures, ~1450°C.

For a clay-rich paste, a linear expansion is observed up to the formation of the first liquid phase and the associated drastic contraction known as liquid-assisted sintering (Fig. 3). The microstructure of a ceramic will not depend on the mean composition, but on that of raw materials, their grain size, and of the firing cycle (heating rate, atmosphere, duration): the fraction of reaction and the nature of formed phases can be thus very variable.<sup>108</sup> The microstructure of the body and the micro- and nano-structure of the glaze constitute the fingerprint of the used technologies.

Briefly we can consider that firing ‘reveals’ the reactivity of the material. Due to the anharmonicity of chemical bond, the bond length increases with temperature; consequently the matter expands quasi linearly with temperature, the thermal expansion coefficient ranging between typically  $10 \times 10^{-7} \text{ K}^{-1}$  (amorphous silica) and  $120 \times 10^{-7} \text{ K}^{-1}$  (metals),<sup>11,34,53,108</sup> values being between 60 and  $100 \times 10^{-7} \text{ K}^{-1}$  for most crystalline oxides. Phase transitions modify the structure of solids and lead to instant contraction or expansion. Therefore, the measurement of the thermal expansion provides information on the nature of the crystalline phases.<sup>11,34</sup> For this reason, a fragment of body in its green state, or already fired in the case of archaeometric studies, can be cut and placed in between a fixed support and a sensor of a dilatometer measuring the displacement of the sample. A quartz-rich mixture shows a huge expansion at 573°C (Fig. 4a), due to the phase transition of quartz, and this event is used by ceramists to measure quartz content in clays, paste and fired body.<sup>11,34</sup> When all the liquid phases have reacted with infusible grains i.e. the material is kinetically stable, the thermal expansion starts again. Reheating a previously fired ceramic specimen will give a linear curve up to the previous firing temperature. As sketched in Fig. 3 the reactions between grains are limited, especially in *terra cotta*, and faience. The reaction is more complete in stoneware and especially in porcelain body, which gives rise to its translucency. Consequently, materials being heterogeneous,

the reactions will start again when the firing temperature will be over over the previous maximal temperature achieved during the firing cycle and the shrinkage develops again. The sintering can be limited or stopped when reactions that lead to expansion take place at the same moment, for instance the formation a new crystalline phase having a less-compact structure or some elements are volatilised.<sup>111</sup> Decarbonation starts around 900 °C, but temperatures up to 1300 °C could be necessary to obtain the complete transformation of coarse grains of a few millimetres because of the phenomenon explained above. It is thus very important to limit the heating rate when reactions take place, e.g. the departure of carbonates in the 900-1100°C temperature range. Fig. 4b compares the thermal expansion measured on different pieces sampled from stoneware<sup>112</sup> and porcelain shards.<sup>113</sup> If a glaze coats the body, the measured thermal expansion is the addition of that of the glaze (a shrinkage jump is observed at ~700 °C in Fig. 4b when the ash-based glaze melt) and of the body (shrinkage above 1200 °C).

The jump at ~200 °C observed during the first heating cycle, but not on cooling, arises from soaked water present in ancient shards excavated from the soil. Cristobalite (a polymorph of silica) phase transition also has event in this temperature range. The main sintering mechanism of pottery is the liquid sintering that induces a drastic shrinkage as exemplified in Fig. 4b: the vertical tangent gives the firing temperature, a vertical tangent being observed when the volume of liquid phase is important, as for porcelain and stoneware. For instance, the sintering temperature of Vietnamese Celadon ranged between 1200 °C and 1300 °C and that of porcelain was ~1350 °C.<sup>38,113,114</sup> *Terra cotta* sinters below 800 °C.<sup>49</sup> This clearly points out that the degree of sintering and associated properties depend on many factors.

**Fig. 5a** sketch shows the thermal expansion of a glass: just before the melting temperature, after the glass transition ( $T_g$ ) a strong expansion takes place (annihilation of the stress) which can be decreased or even vanished by the applied load. The shrinkage is very drastic due to the complete fusion and low viscosity of the glaze. Note, this behaviour depends both on composition and on grinding. If the thermal expansion is measured on a piece where one or two sides are glazed, the measurement will show the behaviour of both materials (proportionally to their thickness). For instance in curve #11+G in Fig. 5 the shrinkage jump at ~700 °C indicates the melting (and firing) temperature of the Celadon glaze.

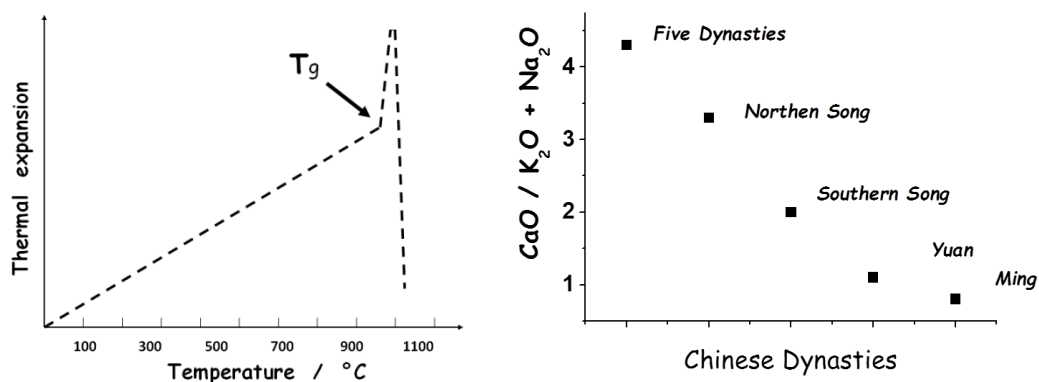


**Fig. 5:** Thermal expansion of a glaze (schematic) showing the melting/glazing temperature; Evolution of the relative CaO content in Chinese porcelain/Celadon glazes from the Five Dynasties (10<sup>th</sup> century) to Ming Dynasty (16<sup>th</sup> century), after<sup>114</sup>.

PbO-SiO<sub>2</sub> glaze composition, the common one of many *terra cotta* glazes, is fired at 900°C (010a Segers cone). The composition can be balanced in order to adapt the thermal expansion, the viscosity, etc.: composition SiO<sub>2</sub>-0.1Al<sub>2</sub>O<sub>3</sub>-0.90PbO-0.05CaO and 0.05 K<sub>2</sub>O need also to be fired at 900°C. If the potter will limit the use of PbO to have a more chemically stable glaze (Pb-rich glazes are dissolved by acetic acid, and hence hazardous), a composition as SiO<sub>2</sub>-0.05B<sub>2</sub>O<sub>3</sub>-0.1Al<sub>2</sub>O<sub>3</sub>-0.1K<sub>2</sub>O-

0.1Na<sub>2</sub>O-0.1CaO-0.5PbO is possible.<sup>34</sup> A composition to be fired at 1300°C (10 Segers cone) will be 6SiO<sub>2</sub>-0.6Al<sub>2</sub>O<sub>3</sub>-0.7CaO-0.3K<sub>2</sub>O. These examples illustrate the complexity of mastering enamelling technology. Fig. 4 shows the evolution of the CaO content versus other flux content with time for Chinese Celadon and porcelain glaze.<sup>114</sup> The decrease of CaO content arise from the replacement of ashes by a mixture of different minerals and is correlated to the increases of the firing temperature and of the mastering of kiln technology.

**Table 4:** Examples of faience compositions<sup>34</sup>

Oxide	Darius Palace* (4th BCE)	Persia* (19th)	Della Robbia* (16th)	Lunéville (18th)	Modern (20th)	Fine (20th)	Vitreous
'H <sub>2</sub> O,CO <sub>2</sub> '	4.36	2.48	8.58				
SiO <sub>2</sub>	90.53	85.17	49.65	67.39	68.0	67.85	70.80
Fe <sub>2</sub> O <sub>3</sub>	0.54	1.26	3.70	2.01	1.0	1.25	0.52
Al <sub>2</sub> O <sub>3</sub>	0.30	1.44	15.50	16.0	10.58	29.40	23.34
TiO <sub>2</sub>	-				1.04		
CaO	3.98	7.29	22.40	13.16	12.72		0.52
MgO	0.04	0.04	0.17	1.02	6.08	0.06	0.15
Na <sub>2</sub> O	0.21	0.2			0.38		4.56
K <sub>2</sub> O					0.25	1.43	

\*: ancient or excavated shards retain water

The mismatch between the thermal expansion of the enamel and the substrate should be controlled,<sup>34,53</sup> with the former being a little lower than that of the substrate to avoid the enamel being put under tension and cracking. However, the stress resistance of glass and ceramic is much higher under compression than under tension. The thermal expansion of the ceramic body being very variable, in particular as a function of quartz content, an huge variety of compositions of glaze have been explored by potters.

Some authors attempt to determine the firing temperature from the presence of specific phases requiring certain temperature to be formed, without taking into account the problem of “*grain size x time x temperature*” conditions required to have a significant (trans)formation of the phases. For ceramics made with coarse grains (2/10 μm or more) this approach is not reliable. As a function of the raw material, the phase formation can be delayed and the conclusions should be considered with caution: for instance carbonates (decarbonation temperature 900 °C) and carbon (combustion temperature 700 °C) may persist in ceramics fired at 1300 °C.<sup>115,116</sup> Likewise, the latter temperature is that required for the reaction between oxygen and carbon atoms in carbide.<sup>117</sup>

### 3.3. Determining the origin of raw materials

Contrarily to gems or even rare metals whose mining places are limited and known for centuries due to their formation under very specific geological conditions, most of the minerals used to make

pottery bodies are rather common. Furthermore, clays are sedimentary detritic rocks, made by mixing different sources. The identification of minor phases and traces is possible but it is often difficult to associate them with a precise quarry when local geology is not known precisely. Nevertheless, analysis of traces and minor phases is useful to categorise groups.<sup>36-38</sup> XRF and ICP-MS easily identify traces such as Rb, Sr, rare earths, uranium, etc.<sup>36-38,65</sup> It has been shown that Raman mapping<sup>41</sup> is more efficient and often faster than XRD to identify minute amounts of specific minerals in ceramic bodies. Due to the large heterogeneity of *terra cotta* and faience (grain size > a few mm) the sampling should be sufficiently large to be representative. Powdering the material guarantees the better homogeneity and representativeness.

Raw materials required to make coloured and opacified enamels should be selected with caution and hence the number of sources is more limited and some minor/major/traces elements associated can be very characteristic.<sup>118-123</sup> Glazes and enamels belong to glassy silicates as glass but, due to the high number of characteristics required, much more than those required for glass objects, the range of compositions experimented by enamel-makers is huge.<sup>124-128</sup> Determining their elemental composition, namely major (~15% or more), minor (1-10%) and trace element (<0.5%), is very useful, but it is very important to consider how representative the composition is in relation with the heterogeneity of the coloured/opacified glass-ceramic.

### 3.4 Analysing the enamels/glazes

If the definition of enamel is “a glassy (silicate) film on a substrate”, the microstructure of the film can be complex: many glazes are a mixture of different amorphous phases (e.g. the *Jun* and ‘*pigeon blood*’ glaze<sup>52,129</sup>) and glazes coloured and opacified with pigments are composite materials, called glass-ceramics.<sup>69</sup> During the glazing, the molten coating reacts with the substrate and forms an interphase (Fig. 2). Furthermore some elements are volatile (B, Pb, Li, Na, etc.) and the surface can have a different composition with respect to the film bulk.

**Fig. 6** shows representative sections of potteries. Porosity of the body can be quantitatively evaluated by measuring the pore size and density by surface unit and compared/calibrated with water absorption measurement (Archimedes method). The combination of optical microscopy and EDS-SEM is efficient for phase identification. Raman microspectrometry identifies both crystalline and amorphous phases.<sup>51,64,126-130</sup> One or more layers coat the body, and in addition an intermediate slip (aqueous suspension of fine white grains, of clays or quartz, typically) can be deposited in between the body and the glaze(s) in order to mask the colour of the body (as made for Iznik ceramic). When sampling is not possible, especially for the study of rare objects, only Raman microspectrometry allows the non-invasive, on-site profile analysis from the surface to a few millimetres, i.e. up to the glaze/body<sup>130</sup> or enamel(patina)/metal interface.<sup>131</sup> Raman profiling is a useful technique to measure the thickness of the coating up to a few hundreds of micron. Note that a carbon film or a crack often forms at metal/coating interface and modifies the Raman intensity.<sup>131</sup> Attaching strips of a conducting carbon-rich tape on the sample section to isolate the spot to be analysed helps to compare data collected by optical techniques (FORS, Uv-vis reflectance, FTIR-ATR & Raman)<sup>92</sup> with SEM-EDS measurement (carbon-rich tape is required if a conducting film has not been deposited).<sup>69,132</sup>

Conservation treatments have been made on many objects, for example archaeological conservators often cover shards with Paraloid<sup>®133</sup> that is detrimental to vibrational analysis. Waxes also cover many objects and agglomerate dust. The latter mixture is also detrimental to the analysis but a good local cleaning can be obtained with a few minutes illumination with blue or green laser beam. In any case, a prior cleaning conducted by a conservator is recommended.

#### *Crystalline phases*

**Table 5** lists the techniques to be used for the identification of phases and their advantages/drawbacks. Sampling points should be distributed on a sufficiently large area, i.e. at least

10 times larger than that of bigger grains, to give representative data. Consequently, measurements on powdered samples by XRD or Raman techniques, or mapping on a large area, are recommended, but not always possible. Due to the molten state of glaze at the firing temperature, the substrate is dissolved at the glaze-body interface and new phases are formed on cooling (Fig. 2).<sup>93</sup> The formed phases are very characteristic of the raw materials and of the firing cycle and this region should be analysed specifically, at different scales. The diffusion coefficient of ions is very variable<sup>108</sup> and depends on the matrix; small size, high charge cations diffuse faster and play an important role in the redox equilibrium in solid and liquid state.<sup>45,55</sup> For instance, as shown in Fig. 6a, the diffusion of the blue colour due to Co<sup>2+</sup> ion paint on the body before deposition of the glaze powder (underglaze décor) is much larger in the glaze (molten at the top firing temperature) than in the porcelain substrate. In Fig. 6d the colour (and colouring cation) diffuses significantly in the fritware substrate, through the glassy phase added to cement the quartz grains.

**Table 5:** Analytical techniques useful for pottery, glass and enamelled artefact studies. References are given as an example.

Methods	Advantages	Drawbacks/Preparation	Best resolution	Information collected	Remarks	Refs
Optical microscopy	Colour identification	Smooth surface required (thin slice for polarization measurement)	0.5 $\mu\text{m}$	Phases, grain & pore size	mobile	35,38,93
SEM-EDS	Large depth of field Large magnification Local composition	Can't see the colour (Very) light elements not measured	>nm	Composition, grain, crystal & pore size		69,93
TEM-EDS	High resolution	Sample preparation, destructive, time consuming	0.1nm	Structure, phase, composition		52,83,86-90
XRD	Phase identification	Smooth surface required	> $\text{mm}^2$	Phase		39-41,52
$\mu\text{XRD}$	Phase identification	Expensive (Synchrotron, Rotating anode)	$\mu\text{m}$	Phase, stress		52,80-91
ICP-MS	High precision	Destructive, representativeness	> $\mu\text{m}$	Elemental composition (major, minor & traces)		65-69,72
XRF	Mobile & fixed instruments	Light elements not measured	>> $\text{mm}^2$		mobile	36,37
$\mu\text{XRF}$	Local analysis	Expensive (Synchrotron, Rotating anode)	$\mu\text{m}$	Local composition		91
LIBS	Erosion - sampling	Micro-destructive Thermal shock	A few $\mu\text{m}$	Composition profile	mobile	73,74
Raman	Mobile, non-invasive No preparation, mapping	Laser selection Not quantitative	0.5 $\mu\text{m}$	Phase, structure, stress, etc. Organic residues	mobile	44,54-64
UV-Vis-NIR	Low cost	Smooth/glossy surface required or polishing	<mm	Colouring agent, site	mobile (FORS)	40,90,92
IR	Low cost, quantitative	Sample preparation	>10 $\mu\text{m}$	Phases, organic residues	mobile	94-102
Thermal expansion	Firing temperature	Sample preparation, destructive	mm	Phase, firing temperature, softening temperature		38,49
DTA/DSC	Melting temperature	Sample preparation, destructive	mm	Phase, melting temperature		106

NAA	Composition Non-destructive	radioactivity	Large volume	Elemental composition (major, minor & traces)	75,76
Ion beam Analysis (RBS,PIXE,PIGE, NRA)	Composition (profile) Non-destructive	Rare facilities, expensive	$\mu\text{m}$	Elemental composition (major, minor & traces)	77-79,107
NMR	residues				99,102
Chromatography	residues				109
Scale	porosity				49,104,105

DTA: Differential Thermal Analysis; DSC: Differential Scanning Calorimetry; EDS: Energy Dispersive Spectroscopy; IR: Infrared transmission/absorption/reflexion; LIBS: Laser Induced Breakdown Spectroscopy; NAA: Neutron Activation Analysis; NIR: Near IR; NRA: Nuclear Reaction Analysis; PIGE: Proton Induced ; PIXE: Proton induced X-ray Emission; Raman: Raman scattering, SEM: Scanning Electron Microscopy; Transmission Electron Microscopy; UV: Ultra-violet analysis; XRD: X-ray diffraction; XRF: X-ray Fluorescence; Vis: visible  $\mu$ :micro.

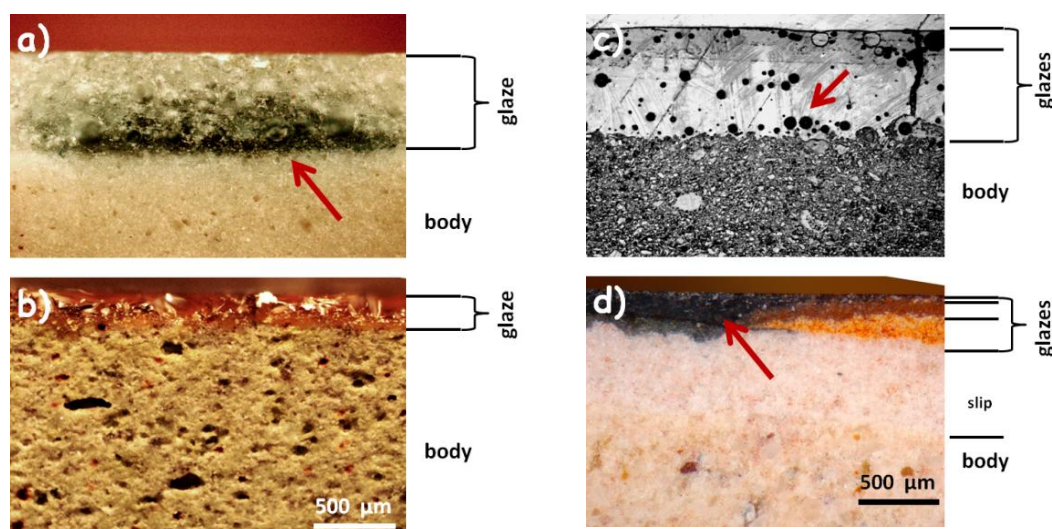


**Fig. 6:** Examples of pottery sections: a, b & d: optical micrographs of sliced shards; c) SEM image of a polished shard; a) Chinese porcelain with a blue underglaze décor (15<sup>th</sup> century); b) terra cotta covered with a lead-rich glaze body (14<sup>th</sup> century, Oman Sultanate); c) Ottoman lead-alkaline multilayer glaze on porous clay-rich body tile tempered with quartz grains (15<sup>th</sup> century); Ottoman Iznik glazed tile: note the thick white quartz grain-rich slip over the body (fritware) and the multilayer glazed blue and red overglaze (16<sup>th</sup> century).

Only transmission electron microscopy (TEM) provides topological information at submicron scale.<sup>52,82-89</sup> Fig. 7 shows some examples. Lustre decor arises from the controlled dispersion of metal nanoparticles in the glaze close to its surface.<sup>45,55,87,88</sup> The alternation of metal nanoparticle-rich and -free layers leads to visible light diffraction phenomenon, dependent on the relative orientations of the observer, the object and the light source. This type of colouration technique is common in the nature (rainbow, opals, beetle carapace, butterfly wing, pulpe skin, etc.) but rare for manmade objects (gratings, advanced optical filter). In the other directions of observation, the colour arises from the light absorption (here by a plasmon, cloud of electrons at the surface of metal nanoparticles).<sup>55</sup> The non-absorbed colour is received by the eyes of the observer. A homogeneous dispersion of copper nanoparticles leads to different red glazes (ox- or pigeon- blood, sacrificial red, etc. as a function of the size, shape, concentration of copper nanoparticles and of the degree of phase separation of the glassy phase)<sup>52</sup> Velvety glaze is obtained by controlling the phase separation in the glaze (two glasses with slightly different compositions, and different optical indices, form in the liquid state and heterogeneity is conserved on cooling (Fig. 6c)).<sup>52,129</sup> In the porcelain body, temperatures above 1250°C lead to the formation of an interconnected array of mullite needles (Fig. 6b, composition:  $3\text{Al}_2\text{O}_3 \cdot 2\text{SiO}_2$ ), that retains the silica-richer molten phase and is the origin of porcelain translucency.<sup>50,52</sup> XRD and Raman microspectrometry easily identify crystalline phases but



only the later technique can characterize the structure of glassy silicates.<sup>134-139</sup> Databases and reference works can be used for band and phase assignment.<sup>64</sup> However, the band intensity of a Raman spectrum depends on many parameters such as laser wavelength, amount of chromophore, crystal orientation, local structure etc. ; consequently databases should be used with caution for the identification of coloured matter. Raman scattering provides a lot of information, but an understanding of the Raman phenomenon is required.

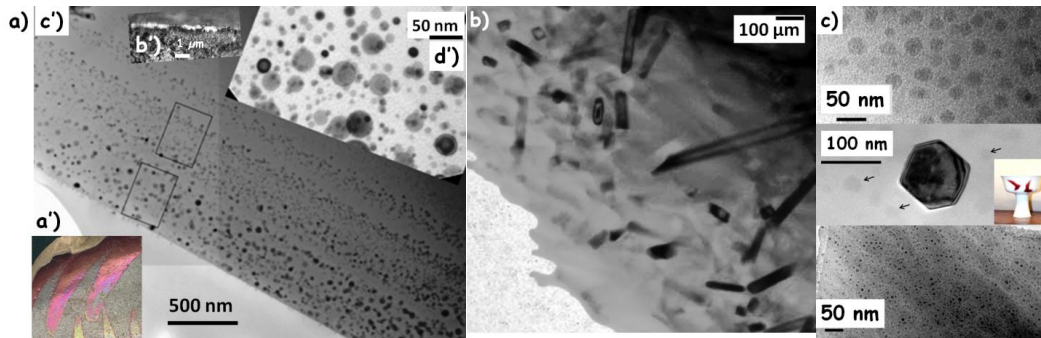


**Fig. 7:** TEM images (Courtesy Ph. Sciau, CEMES-CNRS, Toulouse) of lustre pottery (a), porcelain body (b) and red enamel on porcelain (c) sections; lustre pottery shows iridescent colours (a-a') due to layer alternation with or without metal NPs (c'); only shining is observed by optical microscopy (b'); mullite needles are visible in b); note in c) top the binary phase separation in the red glaze surface and the formation of hexagonal copper crystals (arrows indicate phase separation bubbles); closer to the porcelain substrate a higher density of smaller NPs is observed. See ref.<sup>52</sup> for details.

### Amorphous phases

A large volume of glaze and enamel consists of glassy silicate. Amorphous phases are also present in body such as fritware, vitreous, stoneware and (soft-paste and hard-paste) porcelain. If in most of cases the micron scale is the pertinent resolution to study and identify crystalline phases, a much higher resolution is needed to study the glass and nanocrystalline precipitates. As shown in the TEM image (Fig. 7c), phase separation takes place at the submicron scale<sup>52,129</sup> and hence glaze that looks homogeneous at micron scale is actually heterogeneous. Glaze composition also varies from the top surface (fluxes like Na<sub>2</sub>O, Li<sub>2</sub>O, PbO, B<sub>2</sub>O<sub>3</sub> are highly volatile and easily contaminate the environment) to the centre and the bottom of the glaze (reaction and diffusion in the substrate). Surface composition can be obtained by XRF, SEM-EDS and ICP-MS. In many cases XRF measurements remain qualitative or semi-quantitative because of the difficulty to measure light elements and to control the analysed volume; notwithstanding, the qualitative information obtained is very useful to assign complex Raman spectra. Composition profiles can be obtained by cross-section analysis (fracture or polished section) using SEM-EDS and ion beam analyses or from the top by LIBS abrasion (in Laser Induced Breakdown Spectroscopy a laser pulse volatilizes the matter<sup>73,74</sup> and drill inside from surface to in-depth; caution should be made for enamelled artefact because the huge thermal shock). Vibrational spectroscopy (infrared and Raman scattering) is very effective at identifying glassy phases and in many case can differentiate the contribution of amorphous and crystalline phases.<sup>124-134</sup> FTIR-ATR technique explores the surface layer: the probed in-depth thickness typically ranges between about 2 and 10 μm as a function of the wavenumber range. The technique is thus very efficient to study the corrosion layer if the surface is sufficiently flat. A preparation of the sample is thus often required (powdering, polishing etc.). Note that the low hardness of Ge μATR crystal (20x20 μm<sup>2</sup>, typically) facilitates the contact with a corrugated surface, but promotes its rapid degradation. Crystal should be replaced periodically. Only Raman microspectrometry provides a suitable non-invasive tool to study glassy phases and composites made of both glassy and crystalline phases. Furthermore, mobile instruments are available.<sup>44,54,135</sup> The high efficiency of Raman scattering to study amorphous materials arises from the very local probe of Raman scattering, the polarizability, in other words the variation of the electron distribution across the chemical bond in between atoms.

Consequently, there is no need to have ordering of atoms, but it is necessary to have an electron cloud in between atoms, i.e. to have a covalent bond. The Raman intensity is directly related to the number of electrons involved and almost no spectrum is observed for ionic bonded compounds; the spectrum of just a small amount of carbon (< 1-5 %) can obscure those of major phases.<sup>116,117</sup> For metal, the penetration of light is very limited and special features take places, observed at very low wavenumber range.<sup>35</sup>

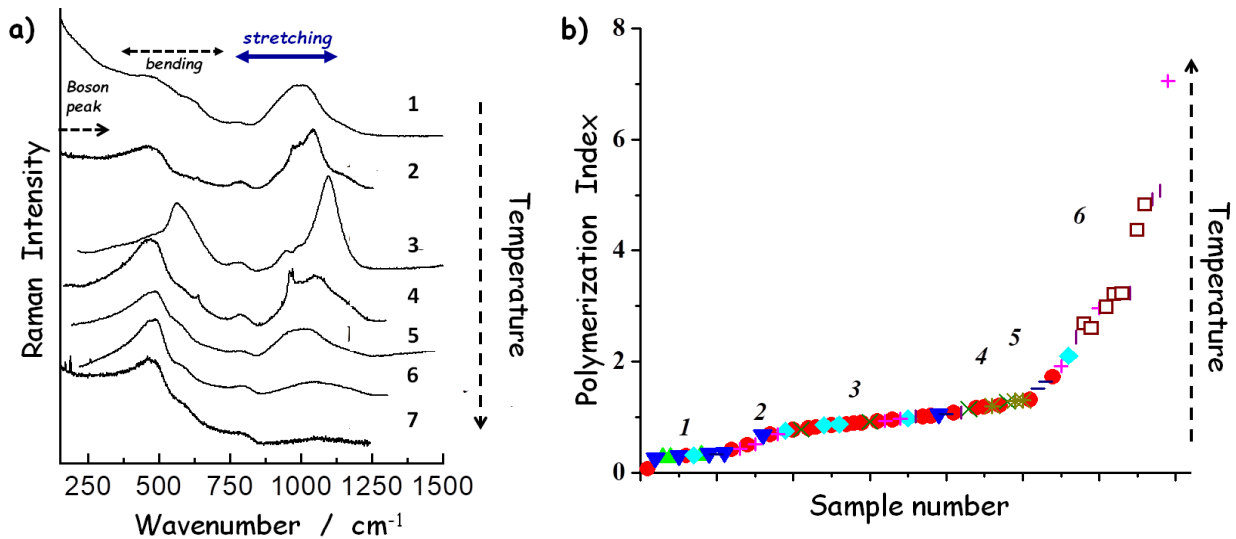


**Fig. 8:** Illustration of the variation of the Raman signature of a selection of glazes (a) and evolution of the ratio of the bending versus stretching band area for series of glazes and glasses (b), after refs<sup>124,126,128</sup>. Typically, the melting temperature ranges from ~600°C to 1450°C.

Since strong covalently-bonded structures have Raman spectroscopic signatures orders of magnitude larger than those of ionic ones, the Raman spectrum of a silicate consists, as a first approximation, solely of the Si-O network signature (Si-O stretching, bending, and librational/collective modes, i.e. the so-called Boson peak).<sup>5,16,39,41</sup> The basic topological and vibrational unit of crystalline and glassy silicate is the SiO<sub>4</sub> tetrahedron. Its tetrahedral (T<sub>d</sub>) geometry is almost unperturbed and the symmetric stretching mode (observed between ~750 and 1200 cm<sup>-1</sup>) is much stronger than the asymmetric ones (same wavenumber range) that could be neglected.<sup>126</sup> Its position varies with the degree of polymerization, i.e. if the Si-O bond is connected to adjacent silicon atom as in pure silica. The second important band arises from the numerous bending modes (observed between 350 and 650 cm<sup>-1</sup>, with E and F characters from the symmetry point of view, that means 2 and 5 bands after symmetry distortion) and from the distribution of librational (hindered rotational) and translational modes (observed below 300 cm<sup>-1</sup>). The latter band, very large and asymmetric is called Boson peak and reflects the short-range structure/disorder. See refs 124-126,134 for a more complete discussion. Consequently, the Raman spectrum of a glassy silicate is the fingerprint of the SiO<sub>4</sub> network. Raman parameters are directly related to the nature and arrangement of the chemical bonds: the stretching mode wavenumber depends on the mechanics (atom mass and bond strength); the bending modes wavenumbers are very sensitive to the bond angle modifications and hence to the environment (presence of fluxing atoms: Pb<sup>2+</sup>, Ca<sup>2+</sup>, Na<sup>+</sup>, K<sup>+</sup>, Li<sup>+</sup> ...). Thus the Raman spectroscopic signature (peak position and intensity) of crystalline and amorphous depends on the silicate nanostructure. It has been demonstrated empirically<sup>124-127</sup> and by Density Functional Theory (DFT) calculation<sup>134</sup> that the area ratio of the bending versus stretching mode provides a good approximation of the degree of polymerization, being very low (<0.5) for glass compositions having a high amount of flux (e.g. PbO-SiO<sub>2</sub> where SiO<sub>4</sub> tetrahedron are mostly isolated), and very high for silica-rich glass and pure silica (>6). The degree of polymerization is directly related to the melting and processing temperature:<sup>121</sup> less Si-O bonds, lower the melting temperature of the composition.

Fig. 8a illustrates the strong variation of the relative intensity of bending and stretching  $\text{SiO}_4$  bands with the modification of the polymerization degree of the Si-O-Si network, from highly polymerized porcelain glaze (#7, where the bending band is very strong) to scarcely polymerized lead-rich terra cotta glaze (#1). Fig. 8b shows the evolution of the bending to stretching mode area ratio for a large number of glass and glaze with various compositions. The highest value is measured for amorphous silica (melting temperature  $\sim 1730^\circ\text{C}$ ) and amorphous alkali and alkali earth aluminosilicates (melting temperature  $>1400^\circ\text{C}$ ). The lowest values are measured for lead-rich glass and glaze melting at temperature less than  $650^\circ\text{C}$ . A similar feature is obtained for crystalline silicates but the curve shows a step-by-step increment with the type of silicate (nesosilicate, inosilicate, cyclosilicates and tectosilicates) whereas a continuous line is observed for glassy silicates in Fig. 8b.<sup>124</sup>

Since the symmetric stretching mode is much stronger than the asymmetric ones, the components of the band can be assigned to the different types of  $\text{SiO}_4$  tetrahedra: isolated ( $Q_0$ ), connected with one ( $Q_1$ ), two ( $Q_2$ ), three ( $Q_3$ ) or full connected ( $Q_4$ ).<sup>44,51,126,128</sup> Miniaturized portable instruments do not exhibit same characteristics that bigger and more expansive fixed instruments available at the laboratory. The replacement of gratings by filter(s) increases the background that should be removed under the control of the operator or automatically by the software. If the recording of narrow bands is easy with portable instruments, having a reliable and robust procedure to subtract the background is not trivial, especially for recovering broad bands. When comparing data obtained with different spectrometers, the same procedures should be used, as exemplified in Fig. 9.<sup>124-128,135</sup> The segmented line shows how the “background” subtraction was done to preserve all contributions (Boson peak and molecular signature of all  $\text{SiO}_4$  tetrahedron forming the aluminosilicate glassy network). Note, the narrow component of nano-crystals dispersed within the glaze have to be considered.

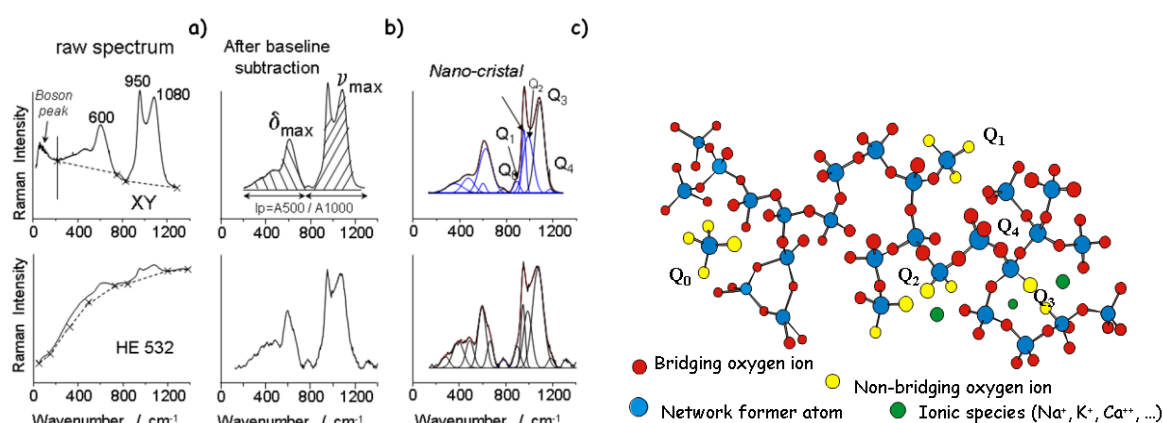


**Fig. 9:** Schematic of the ‘fitting’ procedure for silicate spectra recorded with a high resolution fixed XY Dilor spectrometer measuring up to low wavenumber range (top spectra, Rayleigh elastic scattering at ultra low wavenumber is rejected using holographic gratings) and with a mobile HE532 Horiba instrument with degraded performances below  $200\text{ cm}^{-1}$  (bottom spectra, Rayleigh scattering is suppressed by absorption with an Edge filter); a) as recorded spectra; the dashed line show the separation between the inelastic Raman molecular scattering and the background; b) spectra obtained after background subtraction; the bending and stretching modes of  $\text{SiO}_4$  tetrahedra are observed below and above  $\sim 780\text{ cm}^{-1}$ ; c) the different components arising from isolated ( $Q_0$ ), connected by 1( $Q_1$ ), 2( $Q_2$ ), 3( $Q_3$ ) and 4( $Q_4$ ) oxygen bridging atoms (see the sketch of a incompletely polymerised glass) are shown for the stretching band (reproduced from Ph. Colomban & L.C. Prinsloo, *Optical spectroscopy of silicates and glasses, Spectrosc. Prop. Inorg. Organomet. Compd*, 2009, 40, 128-149, doi:10.1039/b715005a<sup>126</sup>).

A very simple abacus built with the maximal (or band centre of gravity) wavenumber of bending and stretching  $\text{SiO}_4$  bands allows classifying the different types of glass as shown in Fig. 10. Chemometry (principal component analysis, Euclidean cluster classification, etc.) are also useful.<sup>44,126,136,137</sup>

The association of different phases on a substrate leads to interdiffusion at the different interfaces but also to contamination by surface or gas transfer. Atomic diffusion is enhanced at the surface and some fluxes such as PbO, Bi<sub>2</sub>O<sub>3</sub>, B<sub>2</sub>O<sub>3</sub> and Na<sub>2</sub>O, and ions such as Cr and Li, are highly volatile, leading to contamination of the surface of the artefact or of the neighbour artefact. To avoid the contamination each porcelain artefact is put in a ceramic box called saggar. The gaseous atmosphere should be controlled (CO/CO<sub>2</sub>, H<sub>2</sub>/O<sub>2</sub> ratio); this is obtain by controlling the wood water content (green wood), pouring water on coal and opening/closing of air entrance and fume exhaust shutters.

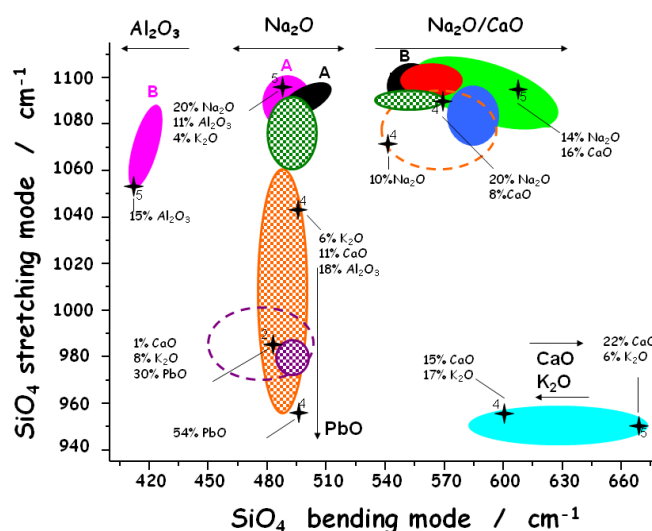


Fig. 10: Plot of SiO<sub>4</sub> stretching vs. bending wavenumber giving the glass type (after <sup>136,137</sup>).

### 3.5 Coloured matter

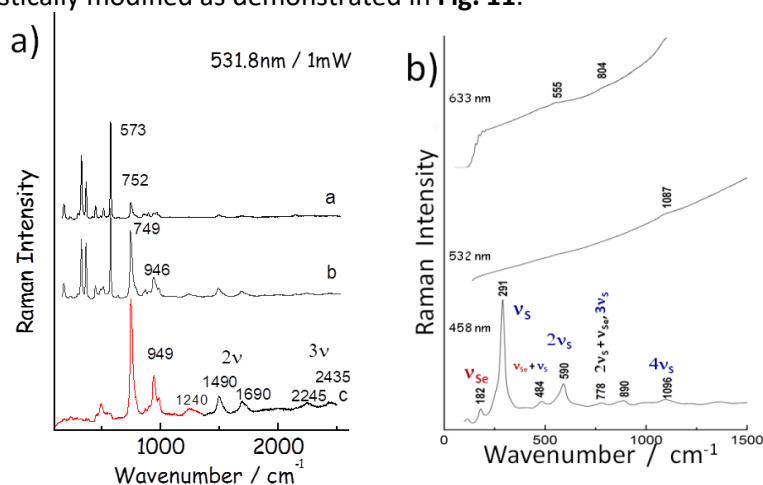
Glass coatings on potteries, glass and metals are applied for technical reasons, namely the tightening of porous bodies and hardening of their surfaces but also for a decorative purpose. Although the coloration of a glass object body is easy undertaken by dissolving as little as a few 0.1% wt of 3d transition metal or 4f rare earth ions, the colouration/opacification of enamels is more complex: an enamel/glaze layer is much thinner (10 to 500 μm, typically) and hence specific colouring agents are needed and their concentration must be higher. To display a high gloss and vivid colour, the dispersion of a 'white' phase in the glaze is useful. XRF technique is a good method to identify colouring agents in a thick homogeneous glass (Table 6). On the contrary, because of the variable and not controllable penetration of the beam, the differentiation of colouring agents in objects covered by many layers of enamel (e.g. Fig. 6d) requires the use of microbeam (μXRF produced by rotating anode X-Ray tube or by Synchrotron Source), and the preparation of the sample through cutting and polishing. The method is however very convenient for the study of surface gilding, even if traces are not visible by eyes.<sup>37</sup> It should be kept in mind that in many cases shards of exceptional artefacts such as those outlined in Table 6<sup>92,121, 136-139</sup> are rarer than some intact objects and hence analytical data very scarce.<sup>136-141</sup> UV-Visible Reflectance and its mobile equivalent technique Fiber Optics Reflectance Spectroscopy (FORS). Both techniques identify very well colouring ions and the symmetry of the occupied site.<sup>39,40,92</sup> Hyperspectral imaging cameras may provide similar information, but the technique is in its infancy for such applications.<sup>142</sup>

Table 6: Examples of on-site studies with mobile Raman/XRF set-ups.

Type	Objects	Date (century)	Place of measurement	Methods	Refs
glass	Ptomelaic enamelled glass beakers (Begram Hoard)	~1 <sup>st</sup> CE	Paris (mnaa-Guimet)	Raman	137
	Enamelled / coloured glass	5th BC - 19th CE	Sèvres (City of		146,148

			Ceramics)	
	Stained glass window	13th-19th CE	Paris (Sainte-Chapelle)France	44,145,147
	Mamluk mosque lamps and bottles	13th-14th CE	Paris (Louvre museum)	137,144
	Brocard and Gallé objects	19th CE	Paris (Fine Art museum)	136
Enamel on metal	Limoges enamels	15th-19th CE		151,152
	Chinese <i>cloisonnés</i>	15th – 19th CE		152,153
Patina	Chinese and Japanese bronzes	10th BC-19th CE	Paris (Cernuschi museum)	131
Pottery	Iznik fritware	15th-16th CE	Sèvres (City of Ceramics)	138
	Kütahya fritware	17th-18th CE		150
	Medici porcelain	16th CE		149
	French soft-paste porcelains (Rouen, St-Cloud, Mennecy, Paris, Sceaux, Chantilly)	17th-18th CE		140,154
	Meissen	18th CE		XRF, Raman 36,37,43
			+ Chicago (Art Institute)	
	Chinese porcelain	16th-19th CE	Paris (mnaa-Guimet)	Raman 132,154

Obtaining a large palette of colours, especially for a material heated at high temperature, requires the use of inorganic pigments.<sup>10,30,53,54</sup> Such pigments are in the crystalline phase, coloured due to with 3d or 4f ions, and stable in molten glass or precipitating on cooling.<sup>53,54</sup> Metals (Au, Cu, Ag) and semi-conductors (CdS-CdSe-X solid solution) nanoparticles are also good pigments.<sup>35,55,88,92</sup> The best analytical technique to identify these pigments is Raman scattering. If the laser colour corresponds to the wavelengths of absorption then resonance Raman spectroscopy takes place: the sensitivity is huge with traces up to micro-mole ( $\mu\text{M}$ ) commonly detected, but the Raman intensity of scattering modes is drastically modified as demonstrated in **Fig. 11**.



**Fig. 11:** a) Comparison between the Raman spectra of tin-based sphene, a and b colourless sphene along two polarisation and c, after 3 wt % chromium doping to obtain the pink pigment; note the peak wavenumbers are almost at the same value but mode involving Sn atoms in interaction with Cr atoms and their combination/overtone bands are enhanced (after<sup>143</sup>); b) Comparison of Raman spectra recorded with red, green and blue laser on a red 'Liberty' stained glass coloured with nanoparticles of CdSe-CdS solid solution (after<sup>92,95</sup>); note the combination/overtone bands.

Fig. 11a compares the spectra recorded on a colourless crystal of sphene (malayite) and a pink one due to Cr doping.<sup>143</sup> The spectrum of the pink pigment looks very different because the modes involving Sn atom coupled with chromium one (forming the chromophore) are enhanced, but their wavenumber is slightly shifted. Obviously, databases<sup>64</sup> are not efficient for many coloured compounds. The observation of overtones ( $2\bar{\nu}$ ,  $3\bar{\nu}$ , etc.) and combination bands demonstrates that

the Raman spectrum is resonant. A good example is the unexpected identification of Lapis Lazuli in many blue enamels,<sup>144</sup> from Ptolemaic period (~3<sup>rd</sup> BC to 1<sup>st</sup> century CE)<sup>137</sup> to Böttger porcelain (18<sup>th</sup> century),<sup>43</sup> including Frederician,<sup>137</sup> Lajvardina<sup>144</sup> and Mamluk<sup>137,145</sup> glass and/or pottery (13<sup>th</sup>-15<sup>th</sup> century). The biggest advantage of Resonance Raman scattering is the huge sensitivity to detect coloured phases that are not detected by other techniques. The ultramarine colour of lapis lazuli is understood to arise from S<sub>n</sub> ions trapped in some sites of feldspar structure. Under blue to red laser illumination, the S<sub>n</sub> ions resonance Raman signature covers the spectrum of the feldspar host matrix, visible only under UV excitation.<sup>119</sup>

Colouring a glass in red is also difficult and the method used by medieval glassmakers<sup>146</sup> was to disperse copper nanoparticles, leads to a huge absorption of the light. Therefore, thin layers of (Cu<sup>0</sup>) metallic copper-containing and -free glass should be deposited alternatively on a colourless glass plate<sup>139</sup> to combine vivid colour and transparency. The contribution of the glass interacting with metal Nanoparticles is enhanced (resonance Raman scattering),<sup>145</sup> which gives a different spectrum from that of the metal nanoparticle-free matrix. Gold (Au<sup>0</sup>) was also used, first by Bernard Perrot, a French-Italian glassmaker<sup>147,148</sup> and then by 18<sup>th</sup> century French and Chinese potters to produce *Camaïeu décor (Cassius' purple)*<sup>140</sup> and *Famille Rose*<sup>132</sup> porcelains, respectively. At the end of the 19<sup>th</sup> century the discovery of CdS-CdSe solid solution with colour ranging from yellow to red allowed the production of red to yellow glass combining vivid colour and a good light transparency.<sup>92</sup> The colour depends both on the composition, on the size and on the concentration of NPs.<sup>90</sup> For red (633 nm) and green (532 nm) laser excitations (i.e. when the laser light doesn't interact with chromophores), the Raman spectrum is that of the glass matrix (more than 98 % volume) (**Fig. 11b**). Using a blue (458 nm) laser, the spectrum shows two modes at ca. 182 and 291 cm<sup>-1</sup> corresponding to symmetric stretching of Cd-Se and Cd-S bonds, respectively, plus combination and overtone modes. The exact wavenumber of the mode depends on the composition.<sup>92</sup>

Cations belonging to glass networks can be exchanged with protons in the presence of moisture, which leads to a degradation of the very surface of glazes and enamels, inducing cracks and loss of optical quality,<sup>144,147</sup> affecting the Raman intensity.<sup>44,64,148</sup> Proton Raman signature and as-recorded Raman intensity can be used for object dating.<sup>44,64,149,152</sup>

### 3.6 On-site study with mobile instruments

Since the beginning of civilisation, emperors, kings and princes have been on the receiving end of exceptionally crafted objects. Furthermore, the fragility and scarcity of many masterpieces has limited the number of surviving objects. Consequently, analytical information on the materials and technologies used to make these precious artefacts is also rare, if not inexistent. For instance, in 1815, H. Davy, – founder of Archaeometric studies with R.A. Ferchault de Réaumur<sup>13,23</sup>- needed large fragments of murals found in Pompeii and pigments of Egyptian blue for their analysis. More recently, in 1922, H.A. Eccles and B. Rackham asked again for several parts of a porcelain service to study the composition of their enamels<sup>13</sup> (analysis who employed solubilisation, specific element precipitation, drying and weighting of the final product). However, present-day ethics require non-destructive, non-invasive techniques. Moreover, the need to keep precious items in secure areas led costly the displacement of artefacts; the use of mobile and contactless instruments is required. The on-going miniaturisation of laser, X-ray sources, spectrometer, detectors and computer led to the popularisation of mobile set-ups and an important increase of their performances.<sup>13 56-64</sup> For instance the identification of lapis lazuli as blue pigment in many glass and glaze in a good example of the potential of the method. Another examples are the identification of Han glass for ear-stopper expected to be in jade and of Arsenic-rich European cobalt in some painted enamelled porcelains made at Qing Court workshop on the guidance of Jesuits,<sup>121</sup> with ores similar to those used in France for soft-paste 17<sup>th</sup>/18<sup>th</sup> century porcelain<sup>159</sup> and for Limoges enamels.<sup>153</sup>



**Fig. 12:** On-site analysis with a mobile Raman set-up. Measurements are made in Museum storage rooms: a) horizontal analysis, b) analysis from the top with a mobile support, c) view of the whole set-up, or d) on the roof of Sainte-Chapelle Palatine Church, Paris;<sup>44</sup> 1, long working distance microscope objective (the distance between the object surface and the front lens is indicated); 2, black textile; 3, paper rams to adjust the height of the object and to suppress vibrations; 4, remote optical head; 5, Raman spectrometer and CCD detector (in blue); 6, laser; 7, computer; e) and f) examples on measurements with an handheld XRF pistol: in e) the screen allows controlling the analysed spot; the instrument gives after collecting data (a few minutes) a first look of the elemental composition.

The availability of a mobile set-up in a museum allows studying many artefacts and collecting unexpected data. For instance the comparison of the nanostructure of enamels covering Chinese *cloisonné* objects<sup>155</sup> with those of Limoges enamels first detect the technology transfer made by Jesuits to Qing workshop.<sup>153,154</sup> Since 2000, series of measurement campaigns have been made with XRF and Raman mobile set-ups. Table 6 lists a selection of studies of enamelled objects, pottery, glass and metal performed with mobile set-ups. Details about the procedure can be found the literature<sup>36-38</sup> (XRF) and<sup>64</sup> (Raman microspectrometry). The main advantage of mobile set-up is the possibility to study all objects without any risks: no contact with last generation of mobile instruments. The specific characteristics of Raman microspectrometry are: i) the high spatial resolution of up to the limit of diffraction of the light (about 0.3  $\mu\text{m}$  using advanced microscope objective and blue laser) on site; ii) penetration depth up to 0.1-10 mm as a function of the transparency; iii) the availability of long working distance objectives with distance to the object surface ranges between  $\sim 13$  mm for  $\times 200$  objective to tens of centimetres or more for low magnification optics; iv) it is possible to perform analysis through a glass cover;<sup>150</sup> v) the good Raman signal for covalent bonded compounds which constitute most of phases found in glass and pottery, including restoration ingredients; and vi) the unique possibility to get information on the structure and composition of amorphous phases. XRF

and Raman measurements provide complementary information.<sup>36-38,141</sup> The main drawbacks of mobile XRF set-ups are: i) the combination of the impossibility to measure light elements with ii) the difficulty to control the in-depth measured volume and the fact that only flat or convex surface can be measured because of the (quasi) contact between the instrument and the analyzed artefact. These weaknesses are almost suppressed by using appropriate procedures: consideration of the elemental ratio is more informative than 'absolute' elemental composition measured by destructive methods such as ICP-MS or LIBS.FORS (Fiber Optics Reflectance Spectroscopy) is a good mobile technique for the identification of colouring agents.<sup>92</sup>

#### 4. Conclusions

The number of publications on the subject is increasing rapidly. Up until 2000, most of the studies were composition analysis of pastes of archaeological samples of Roman, Greek and Islamic origin. Except for the pioneering work conducted by Kingery's MIT Group, by Zhang's Shanghai Institute of Ceramics,<sup>3-6</sup> and by Wood<sup>46</sup> and Tite<sup>155,156</sup> (British Museum/Oxford University), the studies of sophisticated pottery were limited up to the development of non-invasive, mobile XRF and Raman instruments in 2000s. This has led to a rapid increase in the number of studies dedicated to sophisticated enamelled objects, which offers an increasingly better understanding of the connected history of ceramic and pottery technologies and exchanges.

#### 5. Acknowledgments

The author thanks all colleagues and students involved in the studies as well as Institutions and Curators offering the opportunity of studying rare objects and sharing information about them.

#### 6. References

1. Cooper E. (2000) *Ten Thousand Years of Pottery* (4th ed) University of Pennsylvania Press, Philadelphia.
2. Rice PM, *Pottery Analysis. A Sourcebook*, The University of Chicago Press, Chicago, 1987.
3. Kingery W.D. (Ed.) (1984) *Ancient Technology to Modern Science, Ceramic and Civilization Vol. I*, The American Ceramic Society, Columbus.
4. Kingery W.D. (Ed.) 1986a) *Technology and Style, Ceramic and Civilization Vol. II*, The American Ceramic Society, Columbus.
5. Kingery W.D. (Ed.) (1986b) *High Technology Ceramics –Past, Present, and Future. The Nature of Innovation and Change in Ceramic Technology*, Ceramic and Civilization Vol. III, The American Ceramic Society, Westerville.
6. McGovern P.E., Notis M.D., Kingery W.D. (Eds) (1989) *Cross-craft and Cross-Cultural Interactions in Ceramics, Ceramic and Civilization Vol. IV*, The American Ceramic Society, Westerville.
7. Vandiver P.B., Soffer O., Klina B., Svoboda J. (1989) The origin of ceramic technology at Dolni Vestonice Czechoslovakia. *Science*, 246, 1002–1008.
8. Alden J.R., Minc L., Itinerant potters and the transmission of ceramic technologies and styles during proto-Elamites period in Iran, *J. Archaeol. Sci.: Reports* 7 (2016) 863-876.
9. Brongniart A., Riocreux D., *Description Méthodique du Musée de Céramique de la Manufacture Royale de porcelaine de Sèvres*, A. Leleux Libraire-Editeur, Paris, 1845, <http://gallica.bnf.fr/ark:/12148/bpt6k6430171d/f9.image> (accessed 21th December 2017)
10. Brongniart A., *Traité des arts céramiques ou Des poteries considérées dans leur histoire, leur pratique et leur théorie*, Paris, Béchét jeune, A. Mathias, 1844, 3 vols. <http://catalogue.bnf.fr/ark:/12148/cb36023945s.public> (accessed 21th December 2017). Third edition is more complete : 3rd Edition, avec Notes et Additions par A. Salvétat, P. Asselin—Libraire de la Faculté de Médecine, 2 Vol. Paris, 1877.
11. Jouenne C.-A. (2001) *Traité de Céramique et Matériaux Minéraux*, Editions Septima, Paris.



12. Haussone M. (1969) *Technologie Générale. Faïences, Grès, Porcelaines*, Bibliothèque Professionnelle, J-B Baillière & Fils, Paris.
13. Colomban Ph. (2013) The destructive/non-destructive identification of enamelled pottery and glass artifacts and associated pigments – A brief overview, *Arts* 2[3]: 111-123 doi:10.3390/arts2030111.
14. Theophilus (ca. 11<sup>th</sup>-12<sup>th</sup> centuries) *Schedula diversarum artium*. Traduction by Dodwell C.R., Theophilus : the various arts, London (1961).
15. Anonymous, *El Lapidario del Rey Alphonso X*, translation in Spanish by King Alfonso in the year 1279, see in N. Heaton: *J. British Society of Master Glass-Painters* Vol. 48 (1947) p9.
16. Cannella A.-F., *Gemmes, verre coloré, fausses pierres précieuses au Moyen Âge, Le quatrième livre du « Trésorier de Philosophie naturelle des pierres précieuses » de Jean d'Outremeuse*. Bibliothèque de la Faculté de Philosophie et Lettres de l'Université de Liège, Fascicule CCLXXXVIII, Librairie Droz SA, Genève (2006).
17. Abû al-Qâsem Kâshâni, *Arâyes al-javâher*, edited by I. Afshâr, (Teheran, 1966). Translation by J.W. Allan, *Abû'l-Qâsim's Treatise on Ceramics: Iran* Vol. 11 (1973) p111.
18. Porter Y., *Les techniques du lustre métallique d'après le Jowhar-Nâme-ye-Nezâm* (1196), Actes du VIIIe Congrès International sur la Céramique Médiévale en Méditerranée, Thessaloniki, 11-16 October 1999 (Caisse des Recettes Archéologiques, Athènes 2003), p427.
19. Picolpasso C., *Li Tre Libri dell'Arte del Vasaio*, 1557, first translated and edited by C. Popelin, *Les trois Livres de l'Art du Potier*, (Paris, 1881). See also *The Three Book of the Potter's Art*, La Revue de La Céramique et du Verre, Fac-Similé Edition, 2007.
20. Neri A. r.p., *L'Arte Vetraria*, Stamperia de' Giunti, Florence, 1612 (<https://play.google.com/books> accessed 12th January 2018).
21. Macquer M., *Elemens de Chymie-Pratique*. HÉRISANT (J.-T.), vol. 2, Paris (1751). Dictionnaire de Chymie, vol. 2, Didot, Paris (1766, 1777).
22. Lewis W., *Glass and enamel by preparations of gold, commercium philosophicotechnicum; or the philosophical commerce of arts : designed as an attempt to improve arts, trades, and manufactures*. London, p. 170 (1763).
23. Ferchault de Réaumur R.A., *Observations sur la matière qui colore des perles fausses et sur quelques autres matières animales d'une semblable couleur, à l'occasion de quoi on essaie d'expliquer la formation des écailles de poissons*. Mémoires Académie des Sciences, Paris (1716). Idem, *Idée générale des différentes manières dont on peut faire la porcelaine et quelles sont les véritables matières de celle de la Chine*, ibidem (1727). Idem, *Second mémoire sur la porcelaine ou suite des principes qui doivent conduire dans la composition des porcelaines de différents genres et qui établissent les caractères des matières fondantes qu'on ne peut choisir pour tenir lieu de celle qu'on emploie à la Chine*, ibidem (1729). Idem, *Mémoire sur l'art de faire une nouvelle espèce de porcelaine par des moyens extrêmement simples et faciles ou de transformer le verre en porcelaine*, ibidem (1739).
24. Père d'Entrecolle's letters from Ching-te-chen in 1712 and 1722, translated in R. Tichane, *Ching-te-Chen*, New York State Institute for Glaze Research, Painted Post, New York, 1983.
25. Diderot D., d'Alembert J., *Encyclopédie ou Dictionnaire raisonné des Sciences, des Arts et des Métiers*, 1751-1772 (28 vol.) ([encre.academie-sciences.fr/encyclopedie/](http://encre.academie-sciences.fr/encyclopedie/) accessed 12th January 2018).
26. Bastenaire-Daudenart F., *L'Art de fabriquer la faïence*. La Librairie Scientifique et Industrielle, De Mahler et Cie, Paris (1827).
27. Brongniart A., *Mémoire sur la Peinture sur Verre*, Imprimerie Selligue, Paris, 1829.
28. Bontemps G., *Guide du Verrier-Traité historique et pratique de la fabrication des verres, cristaux, vitraux*, Librairie du Dictionnaire des Arts Manufacturés, Paris, 1868.
29. L.A. Salvétat, *Leçons de Céramiques professées à l'Ecole Centrale des Arts et Manufactures*, (Malet-Bachelier, Paris, 1857).
30. Deck Th., *La Faïence*, Maison Quantin, Paris, 1887.

31. Jacquemart A., *Histoire de la céramique*. Librairie Hachette et Cie, Paris (1875).
32. Bertran H, Nouveau manuel complet du Porcelainier, Faïencier, Potier de terre, Encyclopédie-Roret, I. Mulo Libraire-Editeur, Paris, 1898.
33. Bertran H, Nouveau manuel complet de la Peinture sur verre, sur Porcelaine et sur Email, Encyclopédie-Roret, I. Mulo Libraire-Editeur, Paris, 1913.
34. Munier P., *Technologie des Faiences*, Gauthier-Villars, 1957, Paris.
35. Colomban Ph., Truong, A Non-destructive Raman Study of the Glazing Technique in Lustre Potteries and Faiences (9<sup>th</sup>-14<sup>th</sup> centuries) : Silver ions, Nanoclusters, Microstructure and Processing, *J. Raman Spectrosc.* 35 [3] (2004) 195-207.
36. Simsek G., Casadio F., Colomban Ph., Faber K., Bellot-Gurlet L., Zelleke G., Milande V., Moinet E., On-site identification of earlier Meissen Böttger red stonewares using portable XRF: 1, body analysis, *J. Am. Ceramic Society* 97[9] (2014) 2745-2754.
37. Simsek G., Colomban Ph., Casadio F., Bellot-Gurlet L., Faber K., Zelleke G., Milande V., Tilliard L., On-site identification of early Böttger red stonewares using portable XRF/Raman instruments: 2, glaze and gilding analysis, *J. Am. Ceram. Soc.* **2015**; 98[10]: 3006-3013.
38. Simsek G., Colomban Ph., Wong S., Zhao B., Rougeulle A., Liem N.Q., Toward a fast non-destructive identification of pottery: the sourcing of 14<sup>th</sup>-16<sup>th</sup> century Vietnamese and Chinese ceramic shards, *J. Cultural Heritage* 16[2] (2015) 159-172.
39. Ferreira L.F.V., Gonzalez A., Pereira M.F.C., Santos L.F., Casimiro T.M., D.P. Ferreira, D.S. Conceicao, I.F. Machado, Spectroscopy of 16th century Portuguese tin-glazed earthenware produced in the region of Lisbon, *Ceram. Int.* 41 (2015) 13433–13446.
40. Vieira Ferreira L. F., Varela Gomes, M., Pereira, M. F. C.A, Santos L.F., Machado I.F., A multi-technique study for the spectroscopic characterization of the ceramics from Santa Maria do Castelo church (Torres Novas, Portugal), *J. Archaeol. Sci. Reports* 6, 2016, 182-189.
41. Minceva-Sukarova B., Issi A., Raskovska A., Grupce O., Tanevska V., Yaygingöl M., Kara A., Colomban Ph., Characterization of pottery from Republic of Macedonia. III, A study of the comparative mineralogical efficiency using micro-Raman mapping and X-ray diffraction, *J. Raman Spectrosc.* 43[6] (2012) 792–798.
42. Goder W., Schulle W., Wagenbreth O., Walter H., Sonnemann R., Wächtler E., *La découverte de la porcelaine européenne en Saxe*. Meissen, Böttger J.F. (1709-1736), Pygmalion-Gérard Watelet Presse, Paris (1984).
43. Colomban Ph., Milande V., On Site Analysis of the earliest known Meissen Porcelain and Stoneware, *J. Raman Spectrosc.* 2006; 37[5]: 606-613.
44. Colomban Ph., Tournié A., On-site Raman Identification and Dating of Ancient/Modern Stained Glasses at the Sainte-Chapelle, Paris, *J. Cultural Heritage* 8 [3] (2007) 242-256.
45. Colomban Ph. (2016) Natural nanosized raw materials and Sol-Gel technology : the base of pottery since millenniums in Nanosciences and Cultural Heritage, Ph. Dillmann, L. Bellot-Gurlet & I. Nenner Eds, Atlantis Press, 59-74 (DOI : 10.2991/978-94-6239-198-7).
46. Wood N., *Chinese Glazes*, University of Pennsylvania Press, Philadelphia, 1999.
47. Ph. Colomban, A. Tournié, Brother D. de Montmollin, Brother L. Krainhoefner, Vegetable ash as raw material in the production of glasses and enamels, for example the contemporary vegetable ashes from Burgundy, France, <https://arxiv.org/ftp/arxiv/papers/1012/1012.1504.pdf>.
48. The American Ceramic Society, *Phase Diagrams for Ceramists*, (1971), Westerville 15 vol.
49. Colomban Ph., Sagon G., Roche C., Khoi D.N., Liem N.Q., Microstructure and Processing of the Sa Hyunh and Cham Ceramics, *J. Cultural Heritage* 5[2] (2004) 149-155.
50. Carty W.M., Senapatti U., Porcelain-raw materials, processing, phase evolution, and mechanical behavior, *J. Am. Ceram. Soc.* 81(1998)3–20.

51. Colomban Ph., Treppoz F., Identification and Differentiation of Ancient and Modern European Porcelains by Raman Macro- and Microspectroscopy, *J. Raman Spectrosc.* **2001**; *32*: 93-102.
52. Sciau Ph., Noé L., Colomban Ph., Metal nanoparticles in contemporary potters' master pieces: Lustre and red "pigeon blood" pottery: Models to understand the ancient technology, *Ceramics International* *42*[14] (2016) 15349-15357.
53. Epler R.A., Epler D.R., *Glazes and Glass Coatings*, The American Ceramic Society, Westerville, 2000.
54. Colomban Ph., Sagon G., Faurel X., Differentiation of Antique Ceramics from the Raman Spectra of their Colored Glazes and Paintings, *J. Raman Spectrosc.* *32*[5] (2001) 351-360.
55. Colomban Ph. (2009) The use of metal nanoparticles to produce yellow, red and iridescent colour, from Bronze Age to Present Times in Lustre pottery and glass: Solid state chemistry, spectroscopy and nanostructure, *Journal of Nano Research* *8*, 109-132.
56. Vandenabeele P., Edwards H.G.M., Moens L. "A Decade of Raman Spectroscopy in Art and Archaeology". *Chem. Rev.* **2007**; *107*[3]: 675–686.
57. Miliani C., Rosi F., Brunetti B.G., Sgamellotti A., In situ noninvasive study of artworks: the MOLAB multitechnique approach. *Acc. Chem. Res.* **2010** *43*(6):728-38.
58. Colomban Ph., The on-site/remote Raman analysis with portable instruments - A review of drawbacks and success in Cultural Heritage studies and other associated fields, *J. Raman Spectrosc.* **2012**; *43*: 1529-1535.
59. Shackley S. M., Portable X-ray Fluorescence Spectrometry (PXRF): the Good, the Bad, and the Ugly, *Archaeol. Southwest Magazine*, *26* [2] (2012). Retrieved from [www. Archaeologysouthwest.org](http://www.Archaeologysouthwest.org) (accessed May 19, 2014)
60. Vandenabeele P., Edwards H.G.M., Jehlicka J., The role of mobile instrumentation in novel applications of Raman spectroscopy: archaeometry, geosciences, and forensics, *Chem. Soc. Rev.* **2014**; *43*[8]: 2628-2649.
61. Madariaga J.M., Analytical Methods in the field of cultural heritage, *Anal. Methods* **2015**; *7*: 4848, 10.1039/c5ay00072f.
62. Stanzani E., Bersani D., Lottici P. P., Colomban Ph., Analysis of artist's palette on a 16<sup>th</sup> century wood panel painting by portable and laboratory Raman instruments, *Vib.Spectrosc.* **2016**; *85*: 62-70.
63. Vandenabeele P., Donais M.K., Mobile Spectroscopic Instrumentation in Archaeometry Research, *Appl. Spectrosc.* **2016**; *70*[1]: 27-41.
64. Colomban Ph., On-site Raman study of artwork: Procedure and illustrative examples, *J. Raman Spectrosc.* **49**[1] (2018) <http://dx.doi.org/10.1002/jrs.5311>
65. Robertshaw, P., Wood, M., Melchiorre, E., Popelka-Filcoff, R.S., Glascock, M.D., 2010, "Southern African glass beads: chemistry, glass sources and patterns of trade", *Journal of Archaeological Science*, *37*, p. 1898-1912.
66. Koch, J., Günther D., 2011, "Review of the State-of-the-Art of Laser Ablation Inductively Coupled Plasmarometry", *Applied Spectroscopy*, *65* (5), p. 155A-162A.
67. Janssens, K. (Ed.), 2013, *Modern methods for analysing archaeological and historical glass*, J. Wiley & Sons, First Edition, 2 Vol., Chichester, J. Wiley & Sons.
68. Dussubieux L., Golitko M., Gratuze B., *Recent Advances in Laser Ablation ICP-MS for Archaeology*, Springer, Berlin, 2016.
69. Neri E., Morvan C., Colomban Ph., Guerra M. P., Prigent V., Late Roman and Byzantine Mosaic opaque "Glass-ceramics" *Tesserae* (5<sup>th</sup>-9<sup>th</sup> century), *Ceramics International* *42*[16] (2016) 18859–18869.
70. Wolf S., Stos S., Mason R., Tite M.S., Lead Isotope Analyses of Islamic Pottery Glazes from Fustat, Egypt, *Archaeometry* *45*[3], 2003, 405-420.

71. Degryse, P., Schneider, J., 2008, "Pliny the Elder and Sr-Nd isotopes: tracing the provenance of raw materials for Roman glass production", *Journal of Archaeological Science* 35(7), p. 1993-2000.
72. Degryse, P., Henderson, J., Hodgins, G., 2009, *Isotopes in vitreous materials*, Leuven, Leuven University Press.
73. Miziolek, A. W., Palleschi, V., Schechte, I., 2006, *Laser Induced Breakdown Spectroscopy*, Cambridge, Cambridge University Press.
74. Gaudio, R., Dell'Aglio, M., De Pascale, O., Senesi, G. S., De Giacomo, A., 2010, "Laser Induced Breakdown Spectroscopy for Elemental Analysis in Environmental, Cultural Heritage and Space Applications: A Review of Methods and Results", *Sensors*, 10(8), p. 7434-7468.
75. Bonneau A., Moreau J.-F., Auger R., Hancock R. G.V., Émard B., 2014, Analyses physico-chimiques des perles de traite en verre de facture européenne : quelles instrumentations pour quels résultats ? , *Archéologiques* 26, p. 109-132.
76. Sempowski, M.L., Nohe, A.W., Moreau, J-F., Kenyon, I., Karklins, K., Aufreiter, S., Hancock, R.G.V., 2000, On the transition from tin-rich to antimony-rich European white soda-glass trade beads for the Senecas of Northeastern North America", *Journal of Radioanalytical & Nuclear Chemistry*, 244(3), p. 559-566.
77. Poupeau G., Le Bourdonnec F.-X., Carter T., Delerue S., Shackley M.S., Barrat J.A., Dubernet, S., Moretto, P., Calligaro, T., Milic, M., Kobayashi, K., The use of SEM-EDS, PIXE and EDXRF for obsidian provenance studies in the Near East: a case study from Neolithic Catalhayuk (Central Anatolia), *J. Archaeol. Sci.* 37 [11] (2010) . 2705-2720.
78. Padeletti G., Ingo G.M., Bouquillon A., Pages-Camagna S., Aucouturier M., Roehrs S., Fermo P., First-time observation of Mastro Giorgio masterpieces by means of non-destructive techniques, *Appl. Phys. A-Mater. Sci. & Process.* 83[4], 2006, 475-483.
79. Padeletti G., Fermo P., Bouquillon A., Aucouturier M., Barbe F., A new light on a first example of lustred majolica in Italy, *Appl. Phys. A-Mater. Sci. & Process.* 100(3), 2010, p.747-776.
80. Coentro S., Alves, L. C., Relvas, C., Ferreira, T., Mirao, J., Molera, J., Pradell, T., Trindade, R. A. A., Da Silva, R. C., Muralha, V. S. F., The Glaze Technology of Hispano-Moresque Ceramic Tiles: A Comparison Between Portuguese and Spanish Collections, *Archaeometry* 59[4], 2017, 667-684.
81. Pradell T., Molina G., Molera J., Pla J., Labrador A., The use of micro-XRD for the study of glaze color decorations, *Appl. Phys. A-Mater. Sci. & Process.* 111[1], 2013, 121-127.
82. Pradell T., Molera J., Salvado N., Labrador A., Synchrotron radiation micro-XRD in the study of glaze technology, *Appl. Phys. A-Mater. Sci. & Process.* 99[2], 2010, 407-417.
83. Leon Y., Sciau Ph., Passelac M., Sanchez C., Sablayrolles R., Goudeau Ph., Tamura N., Evolution of terra sigillata technology from Italy to Gaul through a multi-technique approach, *J. Anal. Atom. Spectrom.* 30[3], 2015, 658-665.
84. Wang, T., Zhu, T. Q., Feng, Z. Y., Fayard, B., Pouyet, E., Cotte, M., De Nolf, W., Salome, M., Sciau, Ph., Synchrotron radiation-based multi-analytical approach for studying underglaze color: The microstructure of Chinese Qinghua blue decors (Ming dynasty), *Anal. Chim. Acta* 928, 2016, 20-31.
85. Padeletti G., Fermo P., Significant findings concerning the production of Italian Renaissance lustred majolica, *Appl. Phys. A-Mater. Sci. & Process.* 113[4], 2013, 825-833.
86. Pérez-Arantequi J., Molera J., Larrea A., Pradell T., Vendrell-Saz M., Borgia I., Brunetti B.G., Cariati F., Fermo P., Mellini M., Sgamellotti A., Viti C., Luster pottery from the thirteenth century to the sixteenth century: A nanostructured thin metallic film, *J. Amer. Ceram. Soc.* 84 442-446 (2001).
87. Mirguet C., Frederickx P., Sciau Ph., Colomban Ph., Origin of the Self-Organization of Cu<sup>+</sup>/Ag<sup>0</sup> Nanoparticles in Ancient Lustre Pottery. A TEM study, *Phase Transitions* 81 [2-3] (2008) 253-266.
88. Sciau Ph., Nanoparticles in ancient materials: The Metallic Lustre Decorations of Medieval Ceramics, Ch.25, in *Nanotechnology and Nanomaterials "The Delivery of Nanoparticles"*, Hashim A.A. Ed., INTECH, <http://www.intechopen.com/books/the-delivery-of-nanoparticles/nanoparticles-in-ancient-materials-the-metallic-lustre-decorations-of-medieval-ceramics> (accessed 12<sup>th</sup> January 2018).

89. Sciau Ph., Transmission Electron Microscopy: Emerging Investigations for Cultural Heritage Materials, *Advances in Imaging and Electron Physics* 198, 2016, 43-67.
90. Fornacelli C., Sciau Ph., Colomban Ph., CdS<sub>x</sub>Se<sub>1-x</sub> quantum dots as colouring agents of Art Nouveau and contemporary stained glass: a combined transmission electron microscopy and Raman study, *Phil. Trans. R. Soc. A* **2016**; 374: 20160045 (<http://dx.doi.org/10.1098/rsta.2016.0045>).
91. Sciau Ph., Salles Ph., Roucau C., Mehta A., Benassayag G., Applications of focused ion beam for preparation of specimens of ancient ceramic for electron microscopy and synchrotron X-ray studies, *Micron* 40[5-6], 2009, 597-604.
92. C. Fornacelli, Ph. Colomban, I. Turbanti Memmi, Toward a Raman/FORS discrimination between Art Nouveau and contemporary stained glasses from CdS<sub>x</sub>Se<sub>1-x</sub> nanoparticles signatures, *J. Raman Spectrosc.* **2015**; 46[11]: 1129-1139.
93. Maggetti M., d'Albis A., Phase and compositional analysis of a Sèvres soft paste porcelain plate from 1781, with a review of early porcelain techniques, *Eur. J. Mineral* 29[3] (2017) 347-367.
94. Damjanovic L., Bikic V., Saric K., Eric S., Holclajtner-Antunovic I. Characterization of the early Byzantine pottery from Caricin Grad (South Serbia) in terms of composition and firing temperature, *J. Archaeol. Sci.* 46, 2014, 156-172.
95. Memmi Turbanti I., Pottery production and distribution: the contribution of mineralogical and petrographical methodologies in Italy. State of the art and future developments, *Periodico di Mineralogia* 73[3], 2004, 239-257.
96. Bruni S., Guglielmi V., Della Foglia E., Castoldi M., Gianni G. B., A non-destructive spectroscopic study of the decoration of archaeological pottery: from matt-painted bichrome ceramic sherds (southern Italy, VIII-VII BC) to an intact Etruscan cinerary urn, *Spectrochim. Acta Part A-Mol. & Biomol. Spectrosc.* 191, 2018, 88-97.
97. Ostrooumov M., Gogichaishvili A., Raman and Infrared reflection spectroscopic study of pre-Columbian Mesoamerican pottery, *Eur. J. Mineral.* 25[5], 2013, 895-905.
98. Akyuz S., Akyuz T., Basaran S., Bolcal C., Gulec A., Analysis of ancient potteries using FT-IR, micro-Raman and EDXRF spectrometry, *Vibr. Spectrosc.* 48[2] SI, 2008, 276-280.
99. Oudemans T. F. M., Boon J. J., Botto R. E., FTIR and solid-state C-13 CP/MAS NMR spectroscopy of charred and non-charred solid organic residues preserved in roman iron age vessels from the Netherlands, *Archaeometry* 49[3], 2007, 571-594.
100. Raskovska A., Minceva-Sukarova B., Grupce O., Colomban Ph., Characterization of Pottery from Republic of Macedonia, II: Raman and IR Analyses of Glazed Pottery Finds from Skopje Kale, *J. Raman Spectroscopy* 41 [4] (2010) 431-434.
101. Colombini M.P., Giachi G., Modugno F., Ribechini E., Characterisation of organic residues in pottery vessels of the Roman age from Antioe (Egypt), *Microchemical J.*, 79[1-2] 2005, 83-90.
102. Tanasi D., Greco E., Dui Tullio V., Capitani D., Gulli D., Ciliberto F., H-1-H-1 NMR 2D-TOCSY, ATR FT-IR and SEM-EDX for the identification of organic residues on Sicilian prehistoric pottery *Microchem. J.* 135, 2017, 140-147.
103. Mottram H.R., Dudd S.N., Lawrence G.J., Stott A.W., Evershed R.P., New chromatographic, mass spectrometric and stable isotope approaches to the classification of degraded animal fats preserved in archaeological pottery, *J. Chromatogr. A*, 833[2], 1999, 209-221.
104. Kwan Y.B.P., Alcock J.R., The impact of water impregnation method on the accuracy of open porosity measurements, *J. Mater. Sci.* 37[12] 2002, 2757-2761.
105. Waters C., Salih M., Ajinola S., Porosity comparative analysis of porous copper and OOF modelling, *J. Porous Mater.* 22[4], 2015, 989-995.
106. Holakooei P., A technological study of Elamite polychrome glazed brick at Susa, South Western Iran, *Archaeometry* 56[5] (2014) 764-783.

107. Colomban Ph., Calligaro Th., Vibert-Guigue Cl., Liem N. Q., Edwards H.G.M., Accrochage des dorures sur les céramiques et tesselles anciennes, *Rev. Archéométrie-ARCHEOSCIENCES* 29 (2006) 7-20.
108. Kingery w.D., Bowen H.K., Uhlmann D.R., Introduction to Ceramics, 2<sup>nd</sup> Ed., J. Wiley & Sons, New-York, 1976.
109. Colomban Ph., Gel Technology in Ceramics, Glass-Ceramics and Ceramic-Ceramic Composites, *Ceramics International* 15 (1989) 23-50.
110. Coudamy J., Le Feu, les fours, la porcelaine, Gaz de France, Paris (1987).
111. Bruneton E., J. Bigarré, D. Michel, Colomban Ph., Heterogeneity, nucleation, shrinkage and bloating in sol-gel glass ceramics. The case of LAS compositions, *J. Mater Sci.* 32 (1997) 3541-3548.
112. Liem N.Q., Sagon G., Quang V. X., Tan H.V., Colomban Ph., Raman Study of the Microstructure, Composition and Processing of Ancient Vietnamese (Proto)porcelains and Celadons (13-16<sup>th</sup> centuries), *J. Raman Spectrosc.* 31 (2000) 933-942.
113. Liem N.Q., Colomban Ph., Sagon G., Tinh H.X., Hoanh T.B., Microstructure, Composition and Processing of the 15<sup>th</sup> century Vietnamese Porcelains and Celadons, *J. Cultural Heritage* 4[3] (2003) 187-197.
114. Prinsloo L. C., Wood N., Loubser M., Verryn S.M.C., Tiley S., Re-dating of Chinese celadon shards excavated on Mapungubwe Hill, a 13<sup>th</sup> century Iron Age site in South Africa, using Raman spectroscopy, XRF and XRD, *J. Raman Spectrosc.*
115. Osman N., Talib I. A., Hamid H. A., Properties of sol-gel prepared BaCeO<sub>3</sub> solid electrolyte using acetate precursors, *Ionics* 15[2], 2009, 203-208.
116. Havel M., Baron D., Mazerolles L., Colomban Ph., Phonon confinement in SiC nanocrystals: Comparison of the size determination using transmission electron microscopy and Raman spectroscopy, *Appl. Spectrosc.* 61[8], 2007, 855-859.
117. Karlin S., Colomban Ph., Micro-Raman study of SiC fibre-oxide matrix reaction, *Composites Part B*, 29B, 1998, 41-50.
118. Gratuze, B., Soulier, I., Blet, M., Vallauri, L., 1996. De l'origine du cobalt: du verre à la céramique. *Rev. d'Archéométrie* 20, 77-94.
119. Colomban Ph., Rocks as blue (green and black) pigments/dyes of glazed pottery and enamelled glass artefacts – The potential of Raman microscopy, *Eur. Mineralogy J.* **2013**; 25[5]: 863-879.
120. Hancock R.G.V., McKechnie J., Aufreiter S., Karklins K., Kapches M., Sempowski M., Moreau J.F., Kenyon I., Non-destructive analysis of European cobalt blue glass trade beads, *J. Radioanal. Nucl. Chem.* **2000**; 244[3]: () 567–573.
121. Colomban Ph., Zhang Y., Zhao B., Non-invasive Raman analyses of *huafalang* and related porcelain wares. Searching for evidence of innovative pigment technologies, *Ceramics Int.* **2017**; 43: 12079-12088.
122. Giannini R., Freestone I.C., Shortland A.J., European cobalt sources identification in the production of Chinese Famille Rose porcelain, *J. Archaeol. Sci.* **2016**; 80: 27–36.
123. Van Pevenage J., Lauwers D., Herremans D., Verhaeven E., Vekemans B., De Clercq W., Vincze L., Moens L., Vandenaabeele P., A combined spectroscopic study on Chinese porcelain containing ruan-cai colours, *Anal. Methods* **2014**; 6: 387–394.
124. Colomban Ph., Polymerisation Degree and Raman Identification of Ancient Glasses used for Jewellery, Ceramics Enamels and Mosaics, *J. Non-Crystalline Solids* **2003**; 323[1-3]: 180-187.
125. Colomban Ph., Tournié A., Bellot-Gurlet L., Raman Identification of glassy silicates used in ceramic, glass and jewellery: a tentative differentiation guide, *J. Raman Spectrosc.* **2006**; 37[8]: 841-852.
126. Colomban Ph., Prinsloo L.C., Optical Spectroscopy of Silicates and Glasses, in SPECTROSCOPIC PROPERTIES OF INORGANIC AND ORGANOMETALLIC COMPOUNDS, J. Yarwood, R. Douthwaite, S. B. Duckett Eds, RSC Publishing, The Royal Society of Chemistry, 2009, Cambridge pp 128-149.
127. Colomban Ph., Slodczyck A., Raman intensity: an important tool to study the structure and phase transitions of amorphous/crystalline materials, *Optical Materials* **2009**; 31[12] 1759-1763.

128. Colomban Ph., Pottery, Glass and Enamelled Artefacts: How to Extract Information on their Manufacture Technology, Origin and Age? Chapter 8, pp 245-267, in **ANALYTICAL ARCHAEOLOGY**, H.G.M Edwards & P. Vandenberghe Eds, The Royal Society of Chemistry, Cambridge, 2012.
129. Zhu C.X., Wang Y.B., Lu Q., Zhao H.X., Zhu X.L., Fa W.J., Zheng Z., Reproduction of Jun-red glazes with nanosized copper oxides, *J. Am. Ceram. Soc.* 100[10], 2017, 4562-4569.
130. Kock L.D., De Waal D., Raman studies of the underglaze blue pigment on ceramic artefacts of the Ming Dynasty and of unknown origins, *J. Raman Spectrosc.* 38[11], 2007, 1480-1487.
131. Ph. Colomban, A. Tournié, Ph. Meynard, M. Maucuer, On-site Raman and XRF analysis of Japanese/Chinese Bronze/Brass Patina – The search of specific Raman signatures, *J. Raman Spectrosc.* **2012**; 43[6]: 799-808.
132. Ph. Colomban, F. Ambrosi, Anh-Tu Ngo, Ting-An Lu, Xiong-Lin Feng, Stephen Chen, Chung-Lit Choi, Comparative analysis of wucai Chinese porcelains using mobile and fixed Raman microspectrometers, *Ceram. Int.* **2017**; 43(16) 14244-14256.
133. Asquier M., Colomban Ph., Milande V., Raman and Infrared analysis of glues used for pottery conservation treatment, *J. Raman Spectrosc.* 40[11], 2009, 1641-1644.
134. Labet V., Colomban Ph., Vibrational properties of silicates: A cluster model able to reproduce the effect of "SiO<sub>4</sub>" polymerization on Raman intensities, *J. Non-Crystalline Solids* 370 (2013) 10-17.
135. Colomban Ph., On-site Raman identification and dating of ancient glasses: procedures and tools, *J. Cultural Heritage* 9 [Suppl.] (2008) e55-e60.
136. Caggiani M.C., Valloteau C., Colomban Ph., Inside the glassmaker technology: Search of Raman criteria to discriminate between Emile Gallé and Philippe-Joseph Brocard Enamels and Pigment Signatures, *J. Raman Spectroscopy* 45[6] (2014) 456-464.
137. Caggiani M.C., Colomban Ph., Mangone A., Valloteau C., Cambon P., Mobile Raman spectroscopy analysis of ancient enamelled glass masterpieces, *Anal. Methods*, 2013, 5, 4345-4354.
138. Colomban Ph., Milande V., Le Bihan L., On-site Raman Analysis of Iznik pottery glazes and pigments, *J. Raman Spectrosc.* 35 (2004) 527-535.
139. Colomban Ph., Tournié A., Riccardi P., Raman spectroscopy of copper nanoparticles-containing glass matrix: the ancient red stained-glass windows, *J. Raman Spectrosc.* 40[12] (2009) 1949-1955.
140. Mancini D., Dupont-Logié C., Colomban Ph., On-site identification of Sceaux porcelain and faience using a portable Raman instrument, *Ceramics International* 42[13] (2016) 14918-14927.
141. Kirmizi, B., Unsalan O., Bayraktar, K., Colomban Ph., On-site pXRF analysis of glaze composition and colouring agents of "Iznik" tiles at Edirne mosques (15th and 16th-centuries), *Ceramics International* 45 (2019) <https://doi.org/10.1016/j.ceramint.2018.09.213>
142. Sober B., Faigenbaum S., Beit-Arieh I., Finkelstein I., Moinester M., Piasetzky E., Shaus A., Multispectral imaging as a tool for enhancing the reading of ostraca, *Palestine Explor. Quart.* 146[3] (2014) 185-197.
143. X. Faurel, A. Vanderperre, Ph. Colomban, Pink Pigment optimisation by resonance Raman Spectroscopy, *J. Raman Spectrosc.* **2003**; 34[4]: 290-294.
144. Ph. Colomban, Lapis Lazuli as unexpected blue pigment in Lâjvardina ceramics, *J. Raman Spectrosc.* 2003; 34[6]: 420-423.
145. Ph. Colomban, A. Tournié, M.-C. Caggiani, C. Paris Pigments and enamelling/gilding technology of Mamluk mosque lamps and bottle, *J. Raman Spectrosc.* **2012**; 43[12]: 1975-1984.
146. Colomban Ph., Schreiber H., Raman Signature Modification Induced by Copper Nanoparticles in Silicate Glass, *J. Raman Spectroscopy* 36[9] (2005) 884-890.
147. Ricciardi P., Colomban Ph., Tournié A., Milande V., Non-destructive on-site identification of ancient glasses: genuine artefacts, embellished pieces or forgeries ? *J. Raman Spectrosc.* 40 (2009) 604-617.
148. Exhibition Catalogue, 'Bernard Perrot, 1604-1709, Secrets et Chefs-d'oeuvres des verreries royales d'Orléans, Musée des Beaux-Arts, 2010, Orléans

149. Tournié A., Ricciardi P., Colomban Ph., Glass corrosion mechanisms: a multiscale analysis, *Solid State Ionics* 179 (2008) 2142-2154
150. D. Mancini, A. Tournié, M.-C. Caggiani, Ph. Colomban, Testing of Raman spectroscopy as a non-invasive tool for the investigation of glass-protected miniature portraits, *J. Raman Spectrosc.* 2012; 43[2]: 294-302.
151. Colomban Ph., Milande V., Lucas H., On-site Raman Analysis of Medici Porcelain, *J. Raman Spectrosc.* 35[1] (2004) 68-72.
152. Ph. Colomban, R. de Laveaucoupet, V. Milande, On Site Raman Analysis of Kütahya fritwares, *J. Raman Spectroscopy* 36[9] (2005) 857-863.
153. Kirmizi B., Colomban Ph., Blanc M., On-site Analysis of Limoges enamels from 16<sup>th</sup> to 19<sup>th</sup> century, *J. Raman Spectrosc.* 41[10] (2010) 1240-1247.
154. Colomban Ph., Arberet L., Kirmizi B., On-Site Raman Analysis of 17<sup>th</sup> and 18<sup>th</sup> Century Limoges Enamels: Implications on the European Cobalt Sources and the Technological Relationship between Limoges and Chinese Enamels, *Ceramics International* 43[13] (2017) 10158-10165.
155. Kirmizi B., Colomban Ph., Quette B., On-site Analysis of Chinese Cloisonné enamels from 15<sup>th</sup> to 19<sup>th</sup> century, *J. Raman Spectrosc.* 41[7] (2010) 780-790.
156. Colomban Ph., Lu T.-A., Milande V., Non-Invasive on-site Raman study of blue-decorated early soft-paste porcelain: the use of Arsenic-rich (European) cobalt ores – Comparison with *huafalang* Chinese porcelains, *Ceram. Int.*
157. Tite M.S., Pradell T., Shortland A., Discovery, production and use of tin-based opacifiers in glasses, enamels and glazes from the late-iron age onwards: A reassessment, *Archaeometry* 50[1] (2008) 68-84.
158. Tite M.S., Freestone J., Mason R., Molera J., Vendrell-Saz M., Wood N., Lead glazes in Antiquity, Methods of production and reasons for use, *Archaeometry* 40[2] (1998) 241-260.